Åbo Akademi University

Poonam Trivedi

Supramolecular Design of Cellulose-Based Hydrogel Beads

Laboratory of Fibre and Cellulose Technology
Faculty of Science and Technology
Åbo Akademi University
Åbo/Turku 2019

Poonam Trivedi

Born 1984, India

Bachelors in Natural Sciences 2004, KUK, India
Masters in Industrial Chemistry 2006, KUK, India
Pharmaceutical Industry Experience 2007-2013 India
Joined Laboratory of Fibre and Cellulose Technology in Nov 2013

Supramolecular Design of Cellulose-Based Hydrogel Beads

Poonam Trivedi

Laboratory of Fibre and Cellulose Technology
Faculty of Science and Technology
Åbo Akademi University
Åbo/Turku 2019

Supervisor

Professor Pedro Fardim
Laboratory of Fibre and Cellulose Technology
Faculty of Science and Technology
Åbo Akademi University, Finland &
Faculty of Engineering Science
Department of Chemical Engineering
KU Leuven, Belgium

Co-Supervisor

Senior Lecturer Jan Gustafsson
Laboratory of Fibre and Cellulose Technology
Faculty of Science and Technology
Åbo Akademi University, Finland

Reviewers

Professor Monica Ek
Department of Fibre and Polymer Technology
KTH Royal Institute of Technology
Stockholm, Sweden

Professor Zhi-Ming Liu
College of Materials Science and Technology
Northeast Forestry University, Harbin, China

Opponent

Professor Monica Ek
Department of Fibre and Polymer Technology
KTH Royal Institute of Technology
Stockholm, Sweden

ISBN 978-952-12-3789-8 (printed)
ISBN 978-952-12-3790-4 (electronic)
Painosalama Oy – Turku, Finland 2019

To My Family

Preface

The experimental work summarized in this thesis was done in the Laboratory of Fibre and Cellulose Technology during the period from Nov 2013 to Apr 2017, under the supervision of Professor Pedro Fardim and Co-supervision of Senior lecturer Jan Gustafsson. The results are published in peer-reviewed scientific journals and are referred to in the thesis as Papers I-IV, as follows:

I. Trygg, J., Trivedi, P., Fardim, P. (2016). Controlled depolymerisation of cellulose fibres to a given degree of polymerization. *Cellulose Chemistry and Techonology, 5–6*(50), 557–567.

II. Trivedi, P., Trygg, J., Saloranta, T., & Fardim, P. (2016). Synthesis of novel zwitterionic cellulose beads by oxidation and coupling chemistry in water. *Cellulose, 23*(3), 1751–1761.

III. Trivedi, P., Schaller, J., Gustafsson, J., & Fardim, P. (2017). Supramolecular Design of Cellulose Hydrogel Beads. *Journal of Renewable Materials, 5*(5), 400–409.

IV. Trivedi, P., Saloranta-Simell, T., Maver, U., Gradišnik, L., Prabhakar, N., Smått, J. -H., Mohan, T., Gericke, M., Heinze, T., Fardim, P. (2018). Chitosan–Cellulose Multifunctional Hydrogel Beads: Design, Characterization and Evaluation of Cytocompatibility with Breast Adenocarcinoma and Osteoblast Cells. *Bioengineering, 5*(1), 3.

The work compiled in the thesis was a part of the project Future Biorefinery- Products of Renegerated Cellulose funded by TEKES and coordinated by the Finnish Bioeconomy Cluster (FIBIC) and project PShapes funded by Woodwisdom-ERA NET.

Author's contribution

1. The author has performed carbohydrate analysis of the pulps using high performance ion chromatography (HPIC), analysed the data with the main author.

2. The author has concepceptualized the idea of designing zwitterionic system in the pristine cellulose bead, performed functionalization and characterization of the zwitterionic cellulose beads via conductometry, FTIR-Raman spectrometry and wrote the manuscript. The author was also involved in NMR, SEM and ToF-SIMS data analysis.

3. The author has worked from the fundamental idea of blending the CES polymer with the pretreated cellulose to design anionic hydrogel beads. The author has designed and performed all the experimental work except SEM- EDX. The author has also written the manuscript.

4. The author has conceptualized and performed the designing and characterization of multifunctional hydrogel beads except NMR, SEM and biocompatibility experiments. The author was also involved in data anlysis of NMR, SEM and biocompatibility studies and wrote the major part of manuscript with the coauthors.

Supporting publications, presentations and achievements

I. Gericke, M., Gabriel, L., Geitel, K., Benndorf, S., Trivedi, P., Fardim, P., & Heinze, T. (2018). Synthesis of xylan carbonates – An approach towards reactive polysaccharide derivatives showing self-assembling into nanoparticles. *Carbohydrate Polymers, 193*, 45–53.

II. Yildir, E., Sjöholm, E., Preis, M., Trivedi, P., Trygg, J., Fardim, P., & Sandler, N. (2018). Investigation of dissolved cellulose in development of buccal discs for oromucosal drug delivery. *Pharmaceutical Development and Technology, 23*(5), 520–529.

III. Poonam Trivedi, Jani Trygg, Pedro Fardim. A three days course on pretreatment and dissolution of cellulose organized by COSTFP1205 at Friedrich Schiller University of Jena (Germany). 7-9 Apr 2015. Oral and poster presentation.

IV. Poonam Trivedi, Jani Trygg, Pedro, Tiina saloranta, Fardim, Poster presentation in Renewable resources and biorefinery conference held at university of Yorkshire (UK) on synthesis of novel zwitterionic cellulose beads by oxidation and coupling chemistry in water. 3-5 June 2015.

V. Oral and poster presentation on PShapes international collaborative project during COSTFP1205 course and EPNOE conference in Warsaw (Poland). 18 - 22 Oct 2015.

VI. Poonam Trivedi, Jani Trygg, Pedro, Tiina saloranta, Fardim, Poster presentation in Nordic wood biorefinery conference held in Stockholmon (Sweden) on the synthesis of novel zwitterionic cellulose beads by oxidation and coupling chemistry in water. 27-30 Mar 2017.

VII. Received travel grant of 400 Euros from Åbo Akademi University to attend EPNOE 2015 conference.

VIII. Received travel grant of 200 Euros from Åbo Akademi University to attend NWBC 2017 conference.

Contents

Nomenclature

Abbreviations and acronyms

ACS	Amino cellulose sulfate
AFM	Atomic force microscopy
AGU	Anhydroglucopyranose
ATCC CRL-11372	Human bone osteoblast cells
ATR	Attenuated total reflectance
FTIR	Fourier transform infrared
CED	Cupriethylene diamine
CES	Sodium celluloseethylsulfonate
CMC	Carboxymethylcellulose
CNCs	Cellulose nanocrystals
CP MAS	Cross polarization magic angle spinning
DDA	Degree of deacetylation
DMEM	Dulbecco's modified Eagle's medium
DP	Degree of polymerization
DPυ	Viscosity average degree of polymerization
DS	Degree of substitution
EDX	Energy Dispersive X-ray Analysis
FBS	Fetal bovine serum
Girard's reagent T	Carboxymethyl trimethylammonium-chloride hydrazide
hASCs	Human adipose-derived stem cells
HCS	HyCellSolv
HPLC	High-performance liquid chromatography
ILs	Ionic liquids
InGaAs	Indium galliumarsenide
ISO/FDIS	International Organization for- Standardisation Final
LODP	Levelling - off degree of polymerization
MB	Methylene blue
MDA-MB-231	Human breast adenocarcinoma cells
MTT	3-(4,5-dimethylthiazol-2-yl)-2,5 diphenyl tetrazolium bromide
NaClO	Sodium hypochlorite
$NaClO_2$	Sodium chlorite
NaH_2PO_4	Monosodium dihydrogen phosphate dihydrate
PAD	Pulsed amperometric detector
SAXS	Small-angle X-ray scattering
SCAN-Test	Scandinavian Pulp, Paper and Board-Testing Committee
SEC	Size-exclusion chromatography
SEM	Scanning electron microscopy

TEM	Transmission electron microscopy
TEMPO	2,2,6,6-tetramethylpiperidin-1-yl)oxidanyl
ToF-SIMS	Time of flight secondary ion mass spectrometry
VSMC	Vascular smooth muscle cells
WHC	Water holding capacity
XRD	X-ray diffraction

Symbols and Units

%	Percentage
^{13}C	Carbon isotope
^{15}N	Nitrogen isotope
G″	Loss modulus
G′	Storage modulus
Ga^{+}	Gallium ion
pKa	Acid dissociation constant
t	Time
λ	Wavelength
° C	Celsius degree
cm^{-1}	Wavenumber
Hz	Hertz
M	Molar
mL	Millilitre
mM	Milli molar
w	Weight
W	Watt
µl	Microlitre (10^{-6} l)
υ	Frequency of the wave

Abstract

Poonam Trivedi
Supramolecular Design of Cellulose - Based Hydrogel Beads
Doctor of Philosophy in Chemical Engineering Thesis
Åbo Akademi University, Faculty of Science and Technology,
Laboratory of Fibre and Cellulose Technology, Turku 2019.
Keywords: Cellulose, chitosan, depolymerisation, blending, supramolecular, hydrogel beads, oxidation, hydrazide coupling, cytocompatibility, tissue engineering.

The degree of polymerization (DP) of cellulose fibres is an important factor to consider during dissolution in water-based solvent system and to design further advanced biomaterials. The lower is the DP, the higher cellulose concentration solutions can be prepared. Therefore, the DP of the cellulose fibres needs to be controlled. This was achieved by chemical pretreatment of the pulp in which the pKa of the chosen acid and the solvent used had a direct impact on the DP of the treated pulp. Stronger acids resulted in lower DP values of pulp in comparison to weaker acids. Higher ethanol concentration in the treatment solvent mixture lead to the enhanced recovery of the final pretreated pulp.

The pretreated pulp was used to design pristine cellulose beads in 7 % NaOH-12 % Urea-81 % water based solvent system. The cellulose beads were further functionalized into zwitterionic cellulose beads by performing (2,2,6,6-tetramethylpiperidin-1-yl)oxidanyl (TEMPO) mediated oxidation reaction followed by hydrazide coupling. The sodium chlorite ($NaClO_2$)/sodium hypochlorite (NaClO)/TEMPO oxidation system resulted in the generation of carboxylic and carbonyl moieties in the beads. A coupling reaction between the carbonyl and carboxymethyl trimethylammonium chloride hydrazide (Girard's reagent T) resulted in the introduction of cationic moieties in the beads. The molar ratio of the reagents had a crucial role in tailoring carboxylic and carbonyl content generation in the beads. The ultrastructural study of beads showed that zwitterionic beads had larger pores than the pristine cellulose beads.

Anionic cellulose hydrogel beads were designed by blending sodium cellulose ethylsulfonate (CES) an anionic cellulose derivative, with the pretreated cellulose in the 7 % NaOH -12 % Urea - 81 % water based solvent system. The rheology of the blends was studied and the hydrogel beads were coagulated in 2 M sulfuric acid bath. The effect of increasing CES polymer concentration on the hydrogel beads shape, water holding capacity, stability and ultrastructural morphology was studied. The incorporation of CES up to 50 % concentration resulted in stable hydrogel beads with enhanced porosity and water holding capacity.

Functional chitosan-based cellulose hydrogel beads were designed by blending cellulose with chitosan in the sodium hydroxide-urea-water solvent system and consecutive coagulating in 2 M acetic, hydrochloric and sulfuric acid systems. The concentration of chitosan and type of coagulating acid played a decisive role in selecting the hydrogel beads for testing in tissue engineering applications. The hydrogel beads with 70 % chitosan- 30 % cellulose coagulated in acetic acid showed the highest cytocompatibility with breast adenocarcinoma (soft tissue) and osteoblast (hard tissue) cells. The chitosan based hydrogel beads have the potential to be tested further for applications in the field of tissue engineering.

Sammanfattning

Poonam Trivedi
Supramolecular Design of Cellulose – Based Hydrogel Beads (Supramolekulär design av cellulosabaserade hydrogelpärlor)
Avhandling
Åbo Akademi, Fakulteten för naturvetenskaper och teknik, laboratoriet för fiber- och cellulosakteknologi, 2019.
Nyckelord: Cellulosa, kitosan, depolymerisering, blandning, supramolekulär, hydrogel, pärlor, oxidering, hydrazidkoppling, kompatibilitet med celler, vävnadsteknik.

Cellulosans polymerisationsgrad (DP) är en viktig faktor att följa under upplösning av cellulosa i vattenbaserade system vid skapandet av avancerade biomaterial. Ju lägre cellulosans DP är desto högre koncentration av cellulosalösning kan prepareras. Av denna orsak behövs metoder att kunna kontrollera cellulosans DP. Detta åstadkoms genom kemisk förbehandling av cellulosamassan, där pKa av de valda syrorna och själva lösningsmedlet hade en direkt påverkan på DP av den behandlade massan. Starkare syror resulterade i ett lägre DP värde än samma behandling med svarare syror. En högre etanolkoncentration i lösningsmedlet där behandlingen skedde ledde till ett ökat tillvaratagande av den slutliga förbehandlade massan.

Den förbehandlade massan användes till att skapa rena cellulosapärlor i ett vattenbaserat lösningsmedelssystem. Dessa pärlor funktionaliserades till zwitterjoniska cellulosapärlor via en (2,2,6,6-tetrametylpiperidin-1-yl)oxyl (TEMPO)-medierad oxideringsreaktion, vilken följdes av en hydrazidkoppling. Natriumklorit ($NaClO_2$)/natriumhypoklorit (NaClO)/TEMPO oxideringssystemet resulterade i att karboxyl- och karbonylgrupper bildades i pärlorna. En kopplingsreaktion mellan karbonyl och (karboximetyl)trimetylammoniumklorid hydrazid (Girards reagens T) resulterade i att pärlorna erhöll katjoniska grupper. Reagensens molförhållande hade en kritisk roll då man skräddarsydde cellulosapärlornas karboxyl- och karbonylhalt. Ultrastrukturstudier av pärlorna visade att de zwitterjoniska pärlorna hade större porer än de rena cellulosapärlorna.

Anjoniska cellulosapärlor designades genom att blanda natrium cellulosa etylsulfonat (CES), ett anjoniskt cellulsaderivat, med den förbehandlade cellulosan i ett lösningssystem bestående av natriumhydroxid, urea och vatten. Blandningens reologi studerades och hydrogelpärlor koagulerades i ett syrabad innehållande 2 M svavelsyra. Effekten av ökande CES polymer koncentration på hydrogelpärlornas form, kapacitet att hålla vatten, stabilitet och ultrastrukturell morfologi studerades. Genom införandet av CES upp till en halt av 50 % kunde man

producera stabila hydrogelpärlor med förbättrad porositet och kapacitet att hålla vatten.

Funktionella kitosan-cellulosabaserade hydrogelpärlor designades genom att blanda cellulosa med kitosan i lösningssystemet natriumhydroxid-urea-vatten samt därpå följande koagulering i 2 M ättik-, salt- och svavelsyrabad. Kitosankoncentrationen och typen av koaguleringssyra spelade en avgörande roll vid val av hydrogelpärlor för vidare tester till vävnadsteknikapplikationer. Hydrogelpärlorna med 70 % kitosan 30 % cellulosa som koagulerats i ättiksyra visade den högsta cytokompatibiliteten med bröstadenocarcinom (mjuk vävnad) och osteoblastceller (hård vävnad). Kitosanbaserade hydrogelpärlor visade sig ha en potential för vidare forskning för applikationer inom vävnadsteknikfältet.

Objective of the study

The overall aim of this study was to investigate a method for controlled depolymerisation of cellulose pulp and to design and characterize ionic cellulose based supramolecular hydrogel beads in water based solvent system by heterogeneous chemical modification of pristine cellulose beads or by blending functional natural polymers with pretreated cellulose. Further, to expand the scope of material design towards biomedical application, cytocomaptibiltiy and nontoxicity evaluation of the multifunctional hydrogel beads was focused as a first step towards tissue engineering.

Specific Aims

1. Controlled depolymerization of selected pulps in aqueous, ethanolic and mixture of both solvents with varying ratios in relation to the activity coefficient of weak and strong acids (Paper I).
2. Design of functional hydrogel beads by two approaches:
   (i) Heterogeneous chemical functionalization of pristine cellulose beads prepared from pretreated pulp to introduce zwitterionic moieties (Paper II).
   (ii) Blending ionic polysaccharide derivatives with the pretreated cellulose solution followed by regeneration in different coagulating medium. (Paper III) and (Paper IV).
3. The cytocompatibility evaluation of designed chitosan decorated hydrogel beads with breast adenocarcinoma (soft tissue) and osteoblast (hard tissue) cells to find their potential application in the respective tissue engineering (Paper IV).

1. Introduction

The inclination towards the design of natural polymer based hydrogels has always motivated the researchers to design novel functional hydrogels. The fundamental understanding of the natural polymer properties, its dissolution and further shaping into a biomaterial is crucial to design a hydrogel for any application. The dissolution of cellulose was always a challenge in the past, which has been overcome nowadays largely. A wide range of solvents and solvent systems are available, which can dissolve cellulose depending upon their chemical nature. The art of cellulose dissolution in water based solvent systems and regeneration is one of the prime stratergy in designing cellulose-based products such as hydrogels, nano/micro beads. During the dissolution process, the inter and intramolecular hydrogen bonds break, resulting in separation of the cellulose chains. While during the regeneration process, the cellulose chains are self-assembled by non-covalent hydrogen bond interactions. Therefore, the supramolecular forces play a vital role in the designing of the products [1]. The compatibility of cellulose with other cellulose derivatives or polymers in solution state provides an opportunity to design products with desired characteristics. The structures formed after regeneration depends upon the cellulose concentration, nature of the derivative blended in the dope and the regeneration conditions. Therefore, depending upon the need, the cellulose dope concentration can be altered. The cationic or anionic cellulose derivatives or other polymers such as chitosan can be blended with the cellulose. The designed hydrogel can be further transformed into aerogels by lyophilization resulting in preservation of the interconnected structure. Hence we get information about the core morphology of the designed structure.

Significant amount of research has been done in the area of natural polymer based hydrogel design and tissue engineering. Still, until now no one has studied the design and characterization of functional hydrogel beads by blending chemically pretreated cellulose with sodiumcellulose ethylsulfonate (a water-soluble cellulose derivative) and chitosan in the sodiumhydroxide-urea-water-based solvent system or by heterogeneous chemical modification of pristine cellulose beads via oxidation followed by hydrazide coupling chemistry resulting into zwitterionic entities. In continuation of the biomaterial design in the form of hydrogel beads, the cytocompatibility of the chitosan cellulose based hydrogels beads towards breast adenocarcinoma and osteoblast cells was also studied. Hence, the research work compiled in this thesis will provide a new understanding towards the design of cellulose based hydrogels, their properties and feasible potential application in the area of soft and hard tissue engineering.

The thesis is broadly divided into three major sections, (I) Literature overview (II) Experimental and (III) Results and discussion. In the literature overview, cellulose and its chemical structure, the requirement

of pretreatment and the solvents used for cellulose dissolution, cellulose derivatives, modes of designing cellulose-based hydrogels, their characterization and application in tissue engineering is discussed.

The experimental section describes the materials used in the work followed by method of cellulose depolymerization (Paper I), design of zwitterionic cellulose beads (Paper II), sulfonated cellulose based hydrogel beads (Paper III) and chitosan based cellulose hydrogel beads for soft and hard tissue engineering applications (Paper IV). Further, the analytical techniques employed for the characterization of the materials obtained are discussed.

The results and discussion section provides an elaborated discussion about the effect of the conditions employed on the properties of the pulps obtained after pretreatment. Furthermore an insight about the effect of introducing zwitterionic moieties in the cellulose beads and the role of varying reagents ratio is discussed in detail. The effect of blending ionic cellulose CES with cellulose on the rheology and the properties of designed hydrogel beads is provided. Finally, the blending of chitosan with cellulose in water based solvent system, the properties of hydrogel beads coagulated in different coagulating media and the potential application of the hydrogel beads in osteoblasts (hard) and breast adenocarcinoma (soft) tissue engineering are discussed.

2. Literature Review

2.1 An overview of cellulose sources, structure and applications

The biomass produced from the forest resources, agriculture residues and crops is termed as lignocellulosic biomass. It is mainly composed of cellulose, hemicellulose, lignin and pectin along with very low amounts of extractives and inorganics. The composition depends upon the origin and species of the lignocellulosic biomass[2]. For example, hardwood stem is composed of 40–55 % cellulose, 24–40 % hemicellulose, and 18–25 % lignin. On the other hand, the softwood-stem-based materials contain 45–50 % cellulose, 25–35 % hemicellulose, and 25–35 % lignin[3,4]. The separation of lignocellulosic biomass into individual components are required to utilise them for specific desired applications.

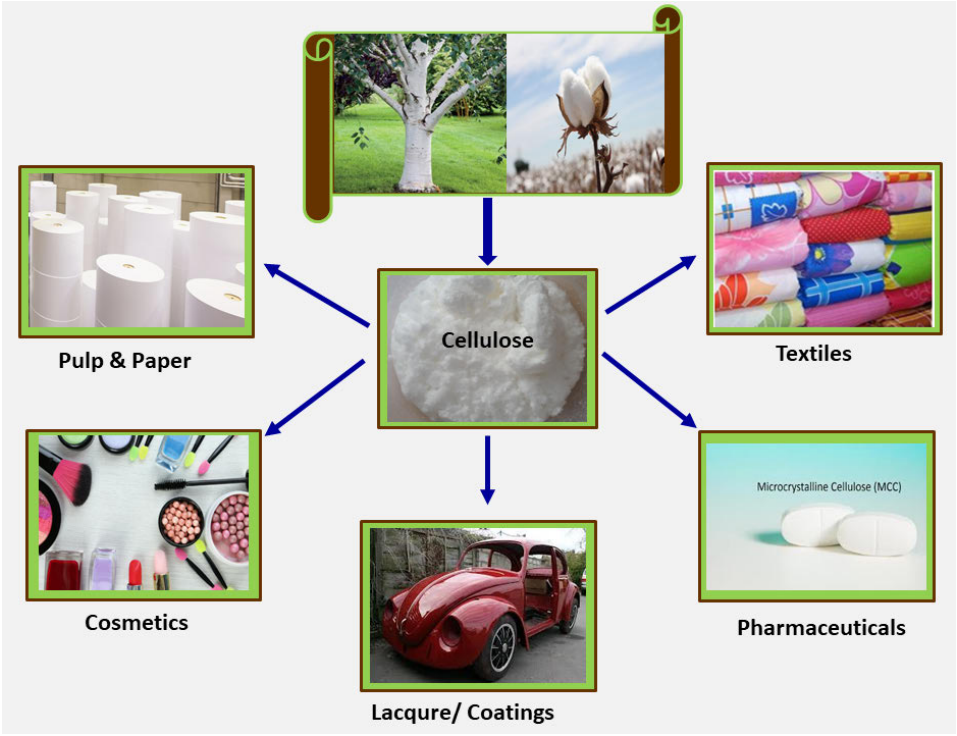

Figure 1. Cellulose sources and the major bulk industrial applications in pulp and paper, pharmaceuticals, textiles, paint and cosmetics.

There are numerous cellulose-based products produced in bulk scale industrially and used in basic commodities such as textiles, cosmetics, pulp

and paper, pharmaceuticals as shown in (Figure 1). Cellulose is one of the prime component and the most abundant polymer on earth with an annual production of 10^{12} tonnes[5]. The french chemist Anselme Payen first discovered the cellulose from a plant source and deduced its chemical formula in 1938[6]. The hypothesis given by Anselme Payen about cellulose that, ''irrespective of source, all celluloses, when freed from other components (or impurities), had one and the same constitution'' was experimentally proved by Emil Heuser. He was also the first to show that some types of oxidized cellulose, when treated with mineral acids, give carbon dioxide, thus indicating that carboxyl groups are present. Staudinger elucidated the macromolecular chemistry of cellulose and was awarded the Noble Prize in 1953 [7]. Cotton is one of the the purest bulk source of natural cellulose with greater than 95 % cellulose content. The dissolving pulp obtained from wood has cellulose content higher than 90 %. The growing research in the field of application-based areas and the establishment of biocompatibility in combination with abundant availability of cellulose has also nailed the chemists, the biochemists, material scientists and medical doctors to focus on new and advanced materials from cellulose for the human race. The possibility of tuning the properties of cellulose by chemical derivatization has provided a base, to develop highly engineered cellulose products[8]. Thus, chemical modification of cellulose is a prerequisite in developing engineered application-based products such as functional hydrogels, crystals, nanoparticles, microparticles, biosensors and textile fibres. Historical and current research has proved that the cellulose biopolymer is a potential candidate for the advanced biocompatible products desired for the civilisation.

Until now four different types of cellulose polymorphs are known and named are as cellulose I, II III, and IV[9]. Cellulose I is present in plants and has crystalline and amorphous regions[10] in which all the strands are parallel and arranged in a highly ordered fashion[11]. It is further divided into two forms cellulose Iα and cellulose Iβ based upon crystal structure. Cellulose Iα has a triclinic unit cell with one chain and cellulose Iβ has a monoclinic unit cell with two parallel chains[12]. The crystal structure of cellulose I is not stable and gets converted into more stable form , the cellulose II during mercerization[13,14] and this process is irreversible. Cellulose II is comparatively more reactive than cellulose I and has been utilized in various applications[15]. For example, cellophane sheets. Cellulose Iβ after liquid ammonia/diamine treatment transforms into cellulose III_I and cellulose II into Cellulose III_{II}. Both the conversions are reversible by Hydrothermal treatment at ~160 °C or Thermal treatment at temperature higher than 200 °C[16,17]. The cellulose IV also has two forms. The cellulose III_I and III_{II} transform into cellulose IV_I and IV_{II} upon heat treatment in glycerol at 260 °C[18]. While reinvestigation of cellulose IV_I structure[19] reveals that it is nothing but a disordered form of cellulose Iβ.

The structure of cellulose biopolymer is a complex hierarchy in which various levels of organisation exist (Figure 2). The highest-level known is the

morphological level consists of micro and nanofibrils corresponding to the architecture. The next is the supramolecular level, which comprises the crystalline and amorphous (disordered) regions concerning the packing and mututal ordering of the macromolecules. The crystalline (highly ordered) and amorphous (disordered) regions in cellulose fibrils are dependent upon the species and biosynthetic procedure. The linear chains in the form of flat ribbons interact with each other through hydrogen bonding and have a strong influence on the chemical behaviour[20–22]. The last level known is the molecular level, in which the pyranose is the single macromolecule of the chain[23].

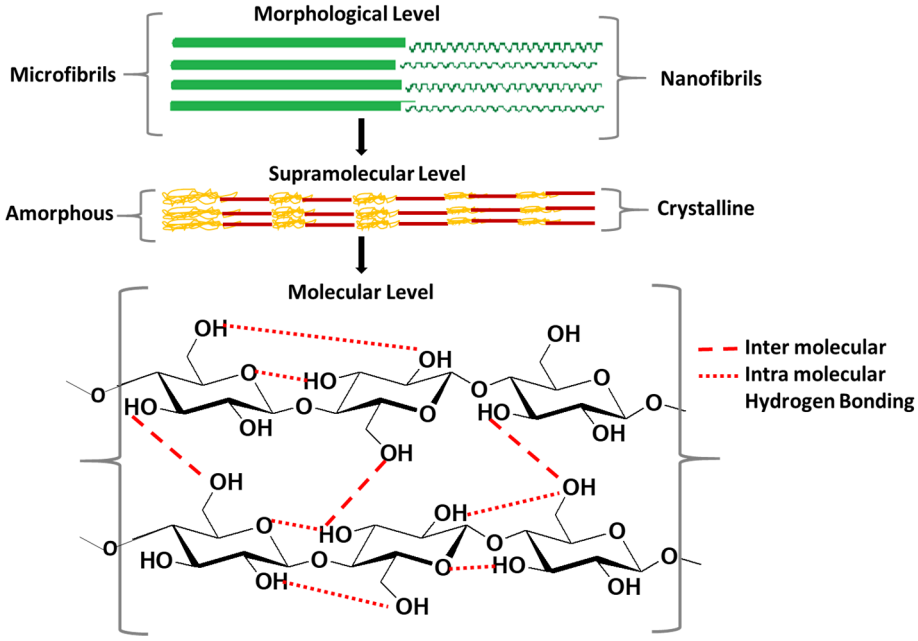

Figure 2. The modified hierarchical depiction of cellulose showing morphological, supramolecular, and molecular level.

At the molecular level, the cellulose consists of linearly arranged D-anhydroglucopyranose units (AGU) linked via β-(1 4) glucosidic covalent bonds. Each repeating AGU possesses three hydroxyl groups, one primary and two secondary. The primary hydroxyl group is present at C-6, and secondary are at C-2 and C-3 positions. There are two types of terminal ends in a cellulose chain. The one in which the C1 hydroxyl is present in hemiacetal form is called reducing end. The second type is the non-reducing, in which C4 hydroxyl group is free and not involved in any linkage. The main cellulose chain is composed of the AGU in which C1 and C4 hydroxyl groups are involved in linkage with the successive AGU'S[24]. The presence of two-fold helical conformations in the crystal structure results in 180° orientation in adjacent molecules and gives stereoregularity to the polymer. There also

exists extensive inter and intramolecular hydrogen bonding, which provides mechanical strength to the fibres. The intramolecular hydrogen bonding is considered to be present between hydroxyl groups of C2, C6 and C3 and the endocyclic oxygen atom[25] and are the major source of stiffness and stabilizes the two fold helical conformation of the cellulose chain. The intermolecular hydrogen bonding occurs between C3-OH of one chain and C6-OH of another chain resulting in interchain cohesion. Along with the hydrogen bonding, van der Waals forces also exist and contribute to the recalcitrance towards dissolution of the cellulose. The structure of cellulose at the macromolecular level is fascinating and decides various properties of cellulose such as solubilization, functionalization. A defined specific DP is required to design cellulose-based hydrogels using water-based solvent systems. Therefore, pretreatment of cellulose is needed before dissolution in the water-based solvent system.

2.2 Cellulose depolymerization for improved dissolution

The dissolution of cellulose in the water-based solvent system is hindered by following factors: higher DP and crystallinity, lower solvent accessibility due to lower porosity, along with hemicellulose and lignin content present[26–28].

Table 1. Various chemical pretreatment methods and the conditions used during the process.

Pretreatment Methods	**Conditions**	**References**
Liquid hot water pretreatment	15 min at temperatures of 200–230 °C	(Mosier *et al.*, 2005), (Mok and Antal, 1992)[30,31]
Weak acid hydrolysis	Dilute (mostly sulfuric) maleic acid, fumaric acid	(Chen *et al.*, 2007)[32] Kootstra *et al.*, 2009)[33]
Strong acid hydrolysis	H_2SO_4 and HCl	(Sun and Cheng, 2002)[34]
Alkaline hydrolysis	Calcium or sodium hydroxide Ammonia	(González Villarreal and Universidad de Guadalajara. Instituto de Botánica.,1986)[35] (Kim and Holtzapple, 2005)[36], (Kim and Lee, 2005)[37]
Organosolv	Ethanol, methanol, acetone, ethylene glycol, up to 200 °C	(Ghose, Pannir Selvam and Ghosh, 1983)[38], (Sun and Cheng, 2002)[34]
Oxidative delignification	Hydrogen peroxide Ozonolysis Wet oxidation	(Sun and Cheng, 2002)[39]
Room Temperature Ionic Liquids (RTIL)	(EMIM)OAc, (EMIM)Cl, (AMIM)Cl, (BMIM)Cl	(Mora-Pale *et al.*, 2011)[40] (Payal *et al.*, 2015)[41]

The dissolving pulp obtained from pulp mills has DP 600-800, which is insoluble in the sodium hydroxide urea water-based solvent system. Thus, to achieve the cellulose dissolution, the reduction in polymeric chain is a necessity. The depolymerisation can be done by various pretreatment methods. In general pretreatment is a process in which hydrolysis of cellulose, hemicellulose, removal of lignin, takes place simultaneously resulting in enhanced surface area and porosity, as well as reduction in crystallinity of cellulose.

The pretreatment processes can be broadly classified into physical or mechanical (milling, ultrasonic pretreatment), chemical (hot water, weak and strong acid hydrolysis, organosolv, oxidative delignification, room temperature ionic liquids), physicochemical (steam explosion, ammonia fibre explosion) and biological pretreatments[29]. Each method has its advantages and drawbacks. An ideal process would result in high yield and low amount of degradation products. The first part of the work in the thesis is related to chemical pretreatment especially acid hydrolysis. Hence, information about the chemical pretreatment methods is provided in (Table 1). In chemical pretreatment of cellulose, the depolymerization occurs due to the chemical reactions, which are initiated by the chemicals used, and the reaction conditions provided. There are various process designed for the chemical pretreatment of cellulose. The acid pretreatment of pulps can be designed in such a way that, the formation of undesired products for instance levulinic acid, and formic acid can be controlled. The choice of acid, the reaction temperature and time certainly has an impact on the levelling off degree of polymerisation (LODP) of the cellulose[42]. Hence cellulose with a low degree of polymerization can be dissolved in water-based solvent system and further transformed into desired forms such as beads, fibres, films[43,44].

2.3 Cellulose Solvents

The polymeric structure of cellulose is a rigid matrix, which requires special kind of solvent system to achieve dissolution. The complexity of the polymeric structure due to the intra and intermolecular hydrogen bonding is a major factor controlling the solubilization in organic or aqueous based solvents. A variety of solvent systems have been explored and applied for the dissolution and regeneration of cellulose. The behaviour of native cellulose fibres, when comes in contact with a liquid was described as follows[45].

1. Swelling of the amorphous region of fibres in the shape of balloons, also known as ballooning effect. The balloon bursts and the fibre dissolves after contact with the solvent system.
2. Only ballooning of the fibre, no further dissolution.
3. Homogenous swelling of the fibre without dissolution.
4. No swelling and no dissolution.

The cellulose solvents are categorised based upon their interaction with cellulose[46]. Therefore the choice of solvent for dissolution and shaping into fibres in the manufacture of textiles, composites or chemical derivatization cellulose for new chemical entities, depends upon the properties of cellulose, conditions applied and the desired product. The cellulose solvents are further categorised as:

1) Derivatizing solvents
2) Non-derivatizing solvents
    a) Ionic Liquids
    b) Organic liquid salt solutions
    c) Aqueous or protic solvents

2.3.1 Derivatizing solvents

Derivatizing solvents are the class of solvents that chemically react with the cellulose, and the intermediate formed is soluble in various solvents. The first cellulose derivative synthesized in this category was cellulose trinitrate, having explosive nature. It is soluble in diethyl ether (non-polar solvent) and ethanol. DMF/N_2O_4 was also a solvent mixture exploited to prepare cellulose nitrate. This solvent system was highly toxic in nature and was discontinued. During that era, another solvent system came into the limelight, which produced an intermediate by the reaction of cellulose with carbon disulphide in aqueous alkali known as cellulose xanthate. This mixture after regeneration in the acidic system leads to the procurement of cellulose of the desired shape. This method was very helpful in spinning fibres from cellulose and was recognised as Viscose process. The drawback of this approach is the generation of highly toxic side products, and malodorous carbon disulfide (CS_2). Another alternative for the Viscose was the carbamate system in which urea is used in aqueous alkaline conditions instead of CS_2.

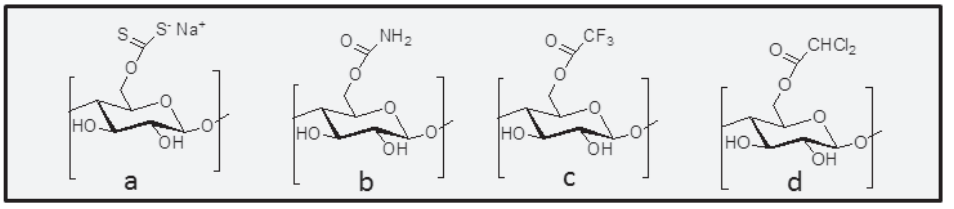

Figure 3. Cellulose intermediates a) Xanthate, b) Carbamate, c) Trifluoroacetate, d) Dichloroacetate

This is known as the CarbaCell process. The most promising and efficient solvent systems in this category are formic acid, acetic anhydride, trifluoroacetic acid. The intermediates formed are well soluble in organic

solvents and the cellulose can be regenerated back after treatment with antisolvent of choice. The cellulose intermediates synthesiszed from the above-mentioned derivatizing solvents are shown in (Figure 3).

2.3.2 Non-derivatizing solvents

The non-derivatizing class of the solvents can dissolve cellulose directly without any stable intermediate formation. The amount of cellulose dissolved very much depends on the solvating strength of the solvent system. For example, organic liquid based salts have higher solvating power than the water-based solvent system. These can be further classified into the following.

Ionic Liquids

Ionic liquids are a class of non-aqueous non-derivatizing solvents, which are composed of alkylated derivatives of aromatic nitrogen-containing metal salts such as ammonium, imidazolium or pyridinium as shown in (Figure 4).

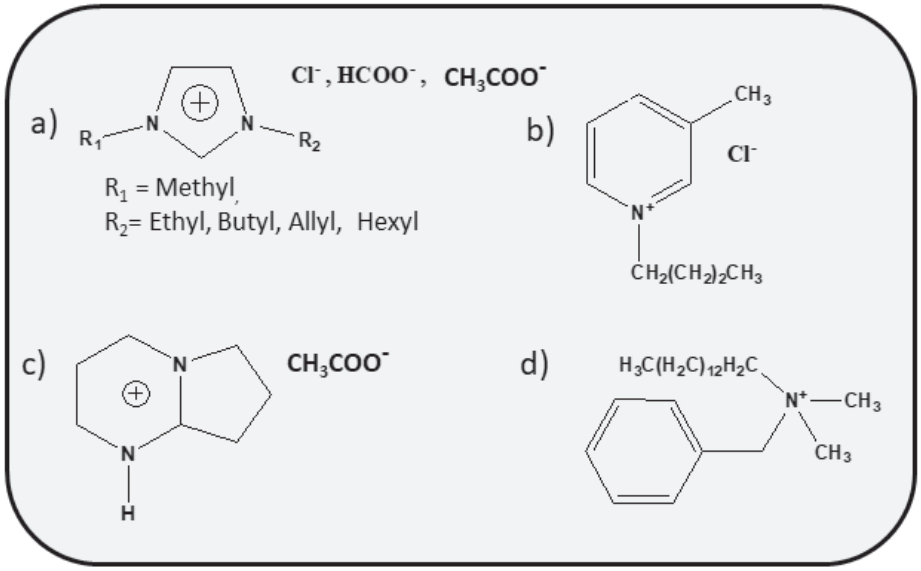

Figure 4. Ionic liquids a) Imidazolium salts, b) Pyridinium salt, c) 1,5 diazabicyclo[4.3.0]non-5-enium acetate ([DBNH] [OAc]), d) Ammonium salt

The high solvating power, dissolution of up to 25 % cellulose, non-volatility, non-inflammability is the surplus of these solvents. It has been elucidated that in ILs only physical solute-solvent interactions play a role in cellulose dissolution[47]. These solvents are highly viscous in nature and have melting points below 150 ^oC. The addition of water, ethanol or acetone in the ionic liquid mixture results in regeneration of the cellulose. The need for ILs with

low viscosity and the low melting temperature is desirable. Recently a new IL named 1,5- diaza bicyclo [4.3.0] non-5-enium acetate ([DBNHH][OAc]) is developed and named as Ioncell-F process[48,49]. This solvent system has provided promising pilot results in the textile manufacturing and has shown the potential for commercialization. The recycling of solvent is desirable to take the procedure for pilot scale applications and to sustain the process. The drawback of ILs is the hygroscopic nature, which retards the efficiency to dissolve cellulose.

Organic liquid salt solutions

Organic liquid salt solutions are polar aprotic solvents, which are also capable of dissolving cellulose up to 18 % with a DP of 800. The most popular solvent system are dimethylacetamide (DMA), dimethyl sulphoxide (DMSO), dimethylformamide (DMF), N- methyl pyrrolidone (NMP) with salts such as lithium chloride (LiCl), lithium bromide (LiBr). The dissolution in organic liquid salt solution occurs due to the interaction of an ion pair with the hydroxyl groups of cellulose. These solvent systems, especially LiCl/DMA are exquisite for homogenous chemical derivatization of cellulose. Another solvent system in this category is N-Methylmorpho-lineoxide-water (NMMO/H_2O). The percentage of water content in NMMO decides the fate of cellulose dissolution. The presence of water up to 17% is acceptable and leads to the dissolution of cellulose by fragmentation. The 19-24 % water results in dissolution of cellulose by ballooning phenomenon and is comparatively slower than the previously mentioned moisture content. Higher moisture content, i.e., more than 25 % will only result in swelling of fibres. The most successful operation for textile fibre production uses the NMMO- H_2O solvent system and is known as Lyocell process[1,50,51]

Aqueous or protic solvents

In these solvent systems, the cellulose is first solvated due to interaction with metal ions. One of the examples are the transition metal salts and amine or ammonium salt based aqueous complexing systems. The mechanism for cellulose dissolution in this system occurs due to the deprotonation of C2 and C3 hydroxyl groups and coordination complex formation with the oxygen. Some common examples are Cuoxen, Nioxen, Zinkoxen[46]. Another class of imperative solvent system is aqueous alkali based solvent systems. The cellulose is soluble in 7- 10 % sodium hydroxide (NaOH) water system below 0 ^{o}C. The degree of crystallinity, and the molecular weight is the decisive factor for dissolution. The aqueous sodium hydroxide is weak solvent to dissolve cellulose with a higher degree of crystallinity and molecular weight. Pretreatment of fibres via enzymatic, chemical or steam explosion is helpful to reduce molecular weight and enhance the solubility.

Another prominent aqueous based solvent system is sodium hydroxide–urea/thiourea. Researchers have shown that 7 % NaOH 12 % urea and 81 % water can dissolve cellulose at -12 ^{o}C[52,53]. In early 90's it was reported that, addition of urea/thiourea to the aqueous sodium hydroxide system enhances the reactivity of cellulose towards xanthation. This observation has always motivated the researchers to find out the exact role of urea in the solvent system. The results obtained from DSC thermograms, ^{13}C,^{15}N and ^{1}HNMR concluded that urea does not interact with sodiumhydroxide and cellulose directly[54,55]. Thus it was proposed that the surface of cellulose–sodium hydroxide complex is enveloped by the hydrated sodium hydroxide, which in turn is bonded to the hydrated urea molecules. The complex is metastable in nature and termed as inclusion complex. The inclusion complex destablizes with time and temperature. It was observed that, even though urea enhances the cellulose dissolution but the temperature and molecular weight of the cellulose are also the governing factors. An increase in cellulose molecular weight and temperature during dissolution strongly decreases the solvent system efficiency[56]. Recently synthesis of water-soluble cellulose tosylates in 7 % NaOH-12 % urea-water system has been reported[57].These solvents are also under investigation for the chemical derivatization of cellulose and are suitable for homogenous etherification of cellulose[58].

The 7 % NaOH 12 % urea and 81 % water solvent system has proven potential to dissolve cellulose. The same solvent had been used to design biomaterials by blending or mixing other polysaccharides such as chitin, chitosan, alginate with cellulose for heavy metal adsorption or as soft electro-sensitive actuators[59,60]. Therefore, the environment friendly nature of the solvent and the simple procedure of designing biomaterials from natural polymers will be an advantage in the research field of biomaterials for biomedical applications.

2.4 Modes of cellulose derivatization and degree of substitution (DS)

To perform the desired functional group modification into the cellulose, the mode of reaction is crucial. The presence of three hydroxyl groups in an AGU and the accessibility of these hydroxyl groups is the deciding factor of cellulose dissolution in any solvent and chemical modification. The chemical derivatization of cellulose can be classified into two modes: (i) Homogenous (ii) Heterogenous.

Homogenous chemical derivatization can be defined as the mode in which all the reactants, comprising cellulose and the reagents are in the same phase as that of the solvent employed or transformation occurs from heterogenous to homogeneous by reactive dissolution in a solvent system. Direct dissolution of cellulose has been achieved in ILs (BMIMCl, AMIMCl)

and organic solvent metal salts (LiCl-DMAC) at certain conditions and desired derivatives are synthesized[61,62]. The homogenous mode of derivatization is comparatively efficient and results in products with higher functionalization[63]. During heterogeneous derivatization, the cellulose is generally solvated by the solvent molecules and the reagents used are soluble. This mode of derivatization is comparatively less efficient than the homogeneous mode, but the recovery of solvent is easier[64]. Heterogenous mode of derivatization has been proved very beneficial in the case of preparation of bio chromatography media for the separation of biomolecules such as proteins and enzymes[65–68]. The degree of substitution (DS) of cellulose can be defined as the number of substituent groups attached to the three-hydroxyl groups per AGU after functionalization. It is a crucial factor, which dictates various properties of cellulose. For example solubility in organic or aqueous solvents, structure formation and biological properties. The historical example is the synthesis of cellulose esters and ethers. Cellulose acetate with DS 0.49 is a water-soluble cellulose derivative while with DS > 1.0, it is organosoluble. The basic concept here can be elucidated that, substitution of hydroxyl groups of cellulose with hydrophobic moieties reduces the hydrophilicity of the cellulose. While substitution of the hydroxyl groups with ionic groups such as quaternary ammonium or sulfonate enhances the hydrophilicity of the biopolymer. The type of chemistry performed and the functional groups introduced significantly decides the performance for applications[69].

2.5 Cellulose Derivatives

Cellulose derivatives are synthesized according to the desired application. As cellulose itself is a hydrophilic polymer, there is a potential to tune its properties such as increased or decreased hydrophilicity by introducing ionic or hydrophobic moieties respectively. The presence of ionic moieties in the cellulose chain results in very specific properties, such as increased water holding capacity. Here we will discuss the ionic derivatives utilized in the thesis work.

2.5.1 Sodium Cellulose Ethyl Sulfonate (CES)

Sulfonated biopolymers such as carrageenan, heparin have been employed in the biomedical field due to the anticoagulant, or antimicrobial properties. The presence of the sulfonate group in these polymers is the key component. Thus, to mimic the properties, sulfonate groups can be introduced into the cellulose by oxa-Michael addition reaction.

In this category, sodium cellulose ethylsulfonate is a derivative, which has been synthesized by reaction of vinyl sulfonate with cellulose under basic conditions. The alkoxide ion generated by the reaction of hydroxyl

groups with sodoum hydroxide, acts as nucleophile and attacks at the β-position in the α-β-unsaturated acceptor i.e vinyl sulfonate.The application of this derivative has been investigated as an absorbent material in case of the wound dressing[70].

2.5.2 Cellulose Carboxylate

The oxidation of hydroxyl groups into a carboxylic group (COOH) results in an anionic character in cellulose biopolymer. The extensively studied method to generate COOH in cellulose and other biopolymers is the TEMPO catalyst mediated oxidation. In this method, the primary hydroxyl group present at C-6 undergoes transformations into intermediates under certain reaction conditions applied and ultimately converts into the carboxylic group. The ease of handling the reaction mass and to obtain cellulose with the desired degree of oxidation has been explored under alkaline, neutral and acidic reaction conditions[71,72]. The TEMPO-mediated approach has also been utilized by researchers to produce nano-fibrillated cellulose. In a recent study, TEMPO-oxidized nano-fibrillar cellulose (ToNFC) macromolecules are transformed into beads via ionotropic gelation in $CaCl_2$. The beads were loaded with OSTEO-1 rat bone cells and had shown to maintain the viability of cells for two weeks. The potential applications in cell therapy and regenerative medicine can be tested further[73]. Similarly, TEMPO-oxidized nanofibres have been utilised as high-density carriers for biomolecules such as small peptides and enzymes[74].

2.5.3 Zwitterionic Cellulose

Cellulose can be derivatized into a special class of derivatives known as zwitterionic cellulose. According to the definition zwitterions have both cationic and anionic species in the same molecule, leading to a total neutral charge, which is seldom possible. Amino cellulose sulfate (ACS) is a zwitterionic cellulose derivative, which has been synthesized in three steps: (i) Synthesis of Tosyl cellulose with a degree of tosylation (DS_{TOS}) between 0.55 and 1.37. (ii) Sulfation of cellulose with SO_3/pyridine complex resulted in the introduction of the sulfate moieties with DS_{Sul} between 1.09 and 1.27. Finally, the tosyl groups at C6 were replaced by nucleophilic amines such as 1,2-diaminoethane and tris-(2-aminoethyl)amine, yielding zwitterionic derivatives[75]. In a recent study, the synthesis of a polyzwitterionic cellulose was achieved by regioselective functionalization. The C-6 position derivatised cellulose carbonate intermediate was treated with a di-tert-butyl dicarbonate (Boc) protected amine, followed by the further introduction of carbonate esters at C-2and C-3 positions. The selective nucleophilic displacement at C-2 with aminoester moiety was followed by the Boc and ester deprotection at C-6 and C-2 respectively. Ultimately, the ammonium group are present at C-6 and carboxylic at C2–C3. The

zwitterionic cellulose coatings have shown an antimicrobial effect against the Gram-negative E. coli bacteria[76, 77].

2.6 Chitosan source, structure and applications

Chitosan is the second largest abundant polymer on earth after cellulose. It is derived after deacetylation of chitin (more than 60 % DDA)[78] and is linear in nature. The major sources of chitosan are crustaceans and fungal mycella[79–81]. A brief pictorial depection of cellulose source, chemical structure and applications are shown in Figure 5. At the molecular level, each D-glucosamine unit has two hydroxyl groups, one primary at C-6, one secondary at C-3 and one amino group at C-2 positions. The amino groups get protonated in diluted acidic aqueous solutions and form ionic complexes with anionic species[82,83]. The amino groups can also form complexes with metal ions, thus used for the recovery of heavy metals from wastewater[84]. Similarly, it can also form complexes with synthetic or natural anionic moieties such as DNA, proteins or lipids [78,85,86].

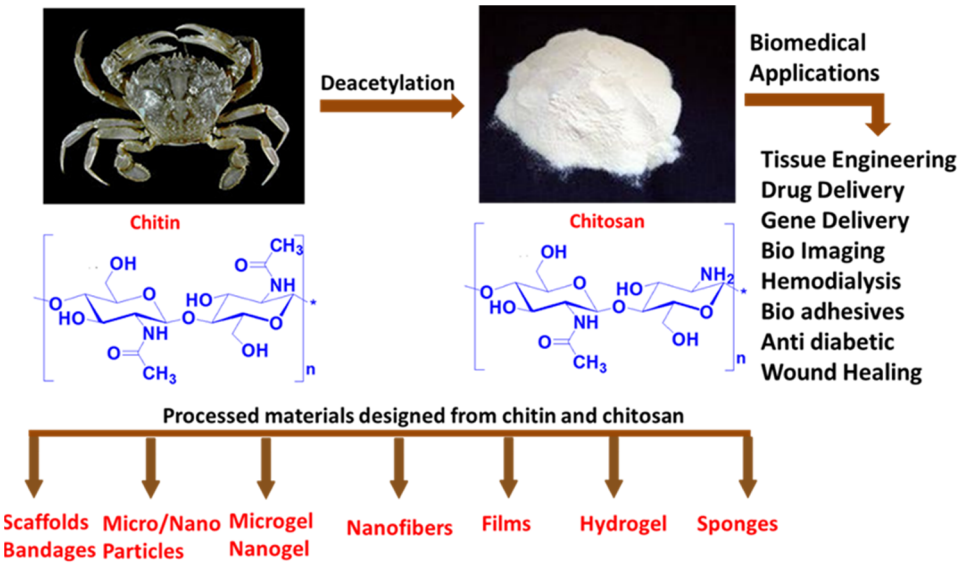

Figure 5. Chitin and chitosan sources, chemical structure and potential application areas.

The chitosan has also shown the properties as antibacterial, antifungal, analgesic, hemostatic and mucoadhesive agent[87–90]. The chitosan due to its remarkable properties has proven to be a potential candidate in the field of tissue engineering. The biomaterial has been used to design hydrogels or scaffolds which can be tested for the attachment and proliferation of desired cell lines[91].

2.7 Cellulose based supramolecular hydrogels

Hydrogels can be defined as a 3D polymer network structures with hydrophilic properties. These can absorb and hold large amount of water via surface tension or capillary effect thus making them suitable for application in the biomedical area[92,93]. The hydrogels can be classified in various ways depending upon their source, size, medium and crosslinking mode[94] as shown in (Figure 6). The gels with predominant crosslinking forces are basically divided into chemical[95,96] and physical gels[97–99] and are also known as supramolecular gels .

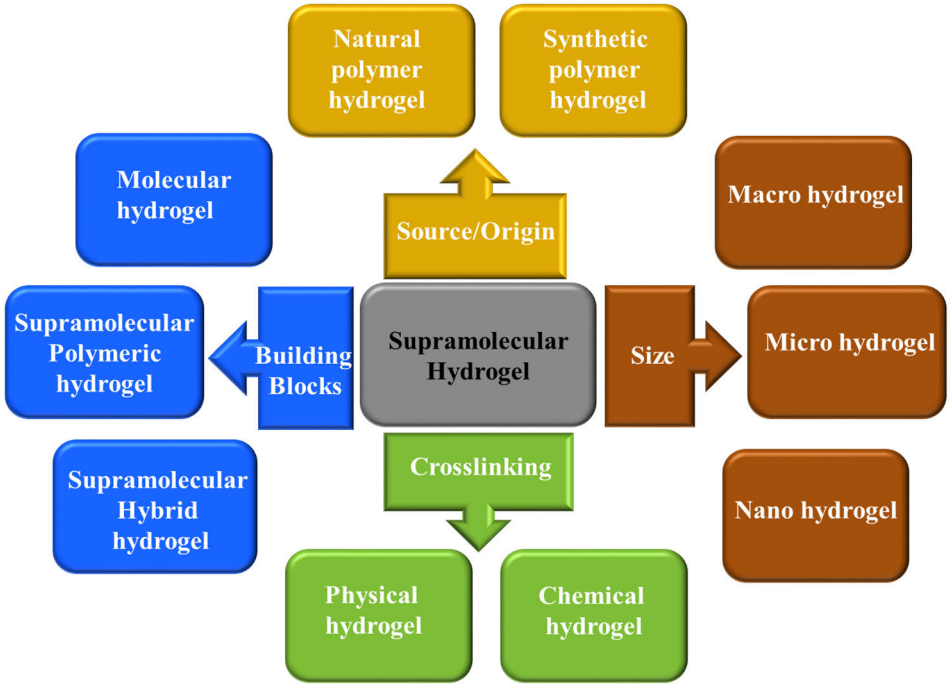

Figure 6. Classification of supramolecular hydrogels based on source, size, crosslinking, and the building blocks.

The chemical gels are stabilized by covalent linkages while in physical gels weak noncovalent interactions such as, metal coordination, hydrogen bonding, π–π stacking, donor–acceptor interactions, host–guest interaction, solvophobic forces (hydrophobic forces for gels in water), and vander Waals interactions play role. Based on size, the supramolecular hydrogels can be classified into i) macro, ii) micro and iii) nanohydrogels. While according to the type of building blocks they are classified into i) molecular hydrogel, ii) supramolecular polymeric hydrogel and iii) supramolecular hybrid hydrogels.

Based upon the source of origin, the gels can also be categorized into synthetic and natural macromolecular gels. Nowadays, the natural hydrogels are gaining importance over the synthetic hydrogels. The hydrogels prepared from natural polymers possess properties such as nontoxicity, bio-compatibility, and biodegradability, which is a prime criteria for the utilization of the hydrogels in the biomedical field[100]. A few examples of polysaccharides used for hydrogels preparation are cellulose, chitosan, dextran, alginate and their derivatives[101–104].

In recent years, cellulose has gained attention due to its promising properties and low production cost[105–108]. Thus, resulting in the application of cellulose-based hydrogels in drug delivery[109], wastewater treatment[110], as reinforcement materials[111], blood purification[112], and as superabsorbent materials in the treatment of edemas[113]. Cellulose obtained from different sources for instance bacterial cellulose, micro fibrillated cellulose, nanocrystalline cellulose or regenerated cellulose can be used to design hydrogels.

The supramolecular hydrogels from the polysaccharides can be designed only after the dissolution in the desired solvent of choice followed by gelation or coagulation. The hydrogels have high water/biological fluid absorbing and retention capacity, which is associated with the hydrophilic nature of the polymer which in turn is governed by the presence of functional moieties in the polymeric chain such as hydroxyl (OH), carboxyl (COOH), amide ($CONH_2$), and sulfonic (SO_3H). In addition, the porosity of the structure also determines the hydrophilicity of the material.

2.7.1 Physical Cellulose Hydrogels

The physical hydrogels are mainly prepared by blending of cellulose with its derivatives or another polymer of choice in a solution state. These are prepared by coagulation or gelation method. The cellulose can be dissolved in an organic solvent system such as DMAc/LiCl or in alkali/(thio)urea aqueous systems. In case of organic solvent systems, the hydrogels in the bead form have been prepared by dropping in a nonsolvent. Suitable organic nonsolvents are for example, methanol or isopropanol. While in the case of aqueous solvent systems, acidic coagulating systems have proved to be one of the best system of choice for the hydrogel beads preparation. The alkali used to dissolve cellulose is neutralized by the acidic medium, thus resulting in reorganization of the inter/intramolecular forces[114]. The properties of the hydrogel beads designed by, either way depends mainly upon the cellulose concentration in the solution, viscosity, molecular weight of the cellulose and the coagulating solvent[115]. The forces playing role in the stabilization of the gels are molecular self- assembly via ionic or hydrogen bond. The hydrogels prepared are highly porous with interconnected network structure. These hydrogels have the potential to be further tested in the biomedical area.

2.7.2 Chemical Cellulose Hydrogels

The chemical hydrogels can be designed by treating a physical hydrogel with a crosslinking reagent during the course of design or after the hydrogels are prepared. The covalent bonds formed between the polymer chains results in the formation of stable structure. The chemical cross linkers for cellulose could be esterifying or etherifying reagent. The esterifying reagents such as carboxylic acids or carboxylic anhydrides results in the formation of –COOR linkages while, the etherifying reagents gives rise to R–O–R linkages amongst the polymer chains. For example, introduction of aldehyde moieties in the polymer can help in crosslinking with other polymer bearing amino, hydrazide or hydrazine moieties[116–119]. The cellulose chemical hydrogels are generally designed to enhance the wet strength of the hydrogels, although the mechanical strength has been enhanced, the water uptake has reduced in these hydrogels.

2.7.3 Composite cellulose hydrogels

The composite cellulose hydrogels are the class of hydrogels, which are prepared by mixing a polymer with another polymer or with inorganic substances. A major reason to design a composite hydrogel is to achieve a hydrogel with the enhanced properties such as increased porosity, water retention capacity for the desired applications. The cellulose composite hydrogels can be classified into (i) natural polymer- based hybrid hydrogels and (ii) biopolymer/synthetic polymer hydrogels and biopolymer/inorganic hydrogels[120]. The cellulose has been blended with carboxymethylcellulose (CMC)[121], sodium alginate (SA)[122], to design hydrogels with ionic functional groups. The presence of functional group, for example -COOH can be utilized to crosslink the polymer chains by adding divalent Ca_{2^+} and or trivalent Al_{3^+} ions in the system during preparation. Similarly synthetic polymers such as polyvinyl alcohol (PVA) and polyethylene glycol (PEG) have been added to the cellulose solutions to design hydrogels[123,124]. The inorganics can also be introduced into the cellulose hydrogels. It can be done by simple mixing of the inorganic material into the cellulose solution[125] or by conversion of the inorganic precursor into the target inorganics in the cellulose solution/suspension[126]. The incorporation of another component into the cellulose hydrogel directly affects the properties as compared to the pristine cellulose hydrogel.

2.8 Characterization of hydrogels

The supramolecular hydrogels can be characterised by various available techniques. Nuclear magnetic resonance (NMR), Fourier transform infrared (FT-IR), and Raman spectroscopy are the main techniques, which can give information about the chemical structure of the hydrogels[127,128]. The

viscoelasticity and gelation time of hydrogels can be studied through modulus rheological methods. Storage (G') and loss moduli (G'') can be used to measure the gelation kinetics of the physical and chemical hydrogels[129]. Other techniques such as SAXS (small-angle X-ray scattering) and XRD (X-ray diffraction) can be used to characterise the nanoscale structure and provide information about the molecular order of the system[129]. The microscopic techniques scanning electron microscopy (SEM), transmission electron microscopy (TEM), atomic force microscopy (AFM) have been used to characterise the morphology and microstructure of hydrogels resulted by rearrangement and formation hydrogen bonds.

2.9 Cellulose-Based Hydrogels in Tissue Engineering

The application of biopolymer-based hydrogels in the field of tissue engineering has now a days gained a lot of interest. In tissue engineering, the focus is to regenerate the malfunctioning tissues/organ. It is achieved by culturing the cells on a natural or synthetic matrix which can mimic the roles of the extracellular matrix and act as a scaffold. The cellulose is regarded as one of the most suitable polymers for tissue engineering due to its nontoxicity, biocompatibility and mechanical properties[130]. The applicability of the cellulose-based hydrogels can be enhanced by blending with other cellulose derivatives such as carboxymethylcellulose (CMC), hydroxypropyl methylcellulose (HPMC) or other natural polymers such as chitosan and hyaluronic acid. The cellulose-based hydrogels have been investigated with the different cell lines. In a study[116], cellulose nanocrystals (CNCs) were employed as nanofillers in a fully biobased strategy for the production of reinforced hyaluronic acid (HA) nanocomposite hydrogels. The human adipose-derived stem cells (hASCs) encapsulated in HA-CNCs hydrogels demonstrated the ability to spread within the volume of gels and exhibited pronounced proliferative activity. In another study, hydrogels of 6-carboxycellulose with 2.1 and 6.6 wt% of COOH groups, were prepared and tested with vascular smooth muscle cells (VSMC) for potential use in tissue engineering. The 6-carboxycellulose with 2.1 wt% of COOH groups showed increased response towards cell colonization. Introduction of chitosan also improved the adhesion and growth of these cells[131]. In another study silanized hydroxypropylmethylcellulose (Si-HPMC) hydrogel with or without calcium phosphate granules was investigated as a potential scaffold for bone tissue engineering[132]. Thus, cellulose based hydrogel have a future in the field of tissue engineering.

3. Experimental

3.1 Materials

Pulps

Dissolving pulp (Enoalfa) supplied from Stora Enso Enocell pulp mill, Finland, was used in all the articles. It is a mixture of birch (*Betula species*) and aspen (*Populus tremula*) with reported properties of 93.5 % alpha cellulose content and viscosity 470 ± 40 ml/g as measured by ISO 5351. The pulp was pretreated according to HyCellSolv pretreatment method to be able to dissolve it in 7 % NaOH-12 %Urea-81 % water system[44]. In Paper I, the following pulps were used for the study: dissolving pulp obtained from Domsjö Fabriker, Sweden (60 % spruce / pine 40 %), bleached kraft pulp of Aspen from MetsäFibre, bleached kraft pulp of eucalyptus and birch from UPM-Kymmene. In paper III, dissolving pulp from Domsjö Fabriker, Sweden was used to synthesize sodium cellulose ethyl sulfonate.

Chemicals

Acetic acid (CH_3COOH), Formic acid (HCOOH), Hydrofluoric acid (HF), Phosphoric (H_3PO_4), Trifluoro-acetic (CF_3COOH), Nitric (HNO_3), Perchloric Hydrochloric acid ($HClO_4$), Hydrochloric acid (HCl, 37 %) were purchased from Merck. Ethanol (92 %) and sodium sulfate (Na_2SO_4, 98 %) were from Sigma-Aldrich. Sodium hydroxide (NaOH) 97 % purchased from Fluka.Urea 99.5 %, sulfuric acid (H_2SO_4) 98 %, monosodium dihydrogen phosphate dihydrate $NaH_2PO_4 \cdot 2H_2O$ 98 %, sodium chlorite ($NaClO_2$) 99 % and carboxymethyl trimethylammonium chloride hydrazide (Girard's reagent T) 99 % were purchased from Sigma Aldrich. (2, 2, 6, 6-tetramethyl-piperidine-1-yl) oxyl (TEMPO) 98 % was obtained from Merck. Sodium hypochlorite (NaClO) 10 % (V/V) solution was purchased from Oy FF-Chemicals AB (Finland). Deionized water from the Milli Q system filtered through 0.2 μm filters was used in all the reactions. 0.1 M NaOH and 0.1 M HCl solutions were prepared from the Titrisol cartridges purchased from Merck, Methionine and Sulphanilamide check standards from Elemental Microanalysis Limited. Low molecular weight chitosan (190–310 kDa with 75–85 % degree of deacetylation) was purchased from Aldrich. MDA-MB-231 cells (Human breast adenocarcinoma), Dulbecco's modified Eagle's medium (DMEM) supplemented with 10 % fetal bovine serum, 2mM L-glutamine, and 1 % penicillin, streptomycin (v/v) were purchased from Life Technologies, ThermoFisher Scientific Inc., Darmstadt Germany. WST-1 cell proliferation reagent was from Roche Diagnostics, Germany. 10 % dimethyl sulfoxide (DMSO), Human bone osteoblasts (ATCC CRL-11372), DMEM with 5 wt. % foetal bovine serum (FBS) were purchased from Life Technologies, ThermoFisher Scientific Inc., Darmstadt, Germany and 3-(4,5-dimethyl-

thiazol-2-yl)-2,5-diphenyltetrazolium bromide (MTT) assay was purchased from Sigma-Aldrich, Hamburg, Germany.

3.2 Methods

3.2.1 Paper I: Pretreatment conditions applied to study the depolymerization of pulps

The effect of pretreatment conditions on the controlled depolymerization of pulps was studied. The HyCellSolv (HCS) pretreatment was performed as a reference experiment, in which 100 mL ethanol (92.5 %) was preheated to 75±1 °C followed by the addition of 4.0 mL of 37 % HCl (~48 mmol) into the reaction vessel. 10 g pulp of equal sized pieces was added and treated for 2 h. The reaction mass was cooled to room temperature, then filtered and washed with distilled water until neutral pH was achieved. The pulp was dried in an oven at 60 °C. The effect of the acidic strength of the acids mentioned in Table 2 was studied on the five different pulps as mentioned in Table 5.

Table 2. Acids used for pulps depolymerization and their pKa values.

Acid Used	**pKa**
[1]Acetic (CH_3COOH)	4.76
[1]Formic ($HCOOH$)	3.75
[1]Hydrofluoric (HF)	3.20
[1]Phosphoric (H_3PO_4)	2.16
[1]Trifluoro-acetic (CF_3COOH)	0.52
[2] Nitric (HNO_3)	-1.4
[3]Sulfuric (H_2SO_4)	-2
[3]Hydrochloric (HCl)	-7
[1]Perchloric ($HClO_4$)	-10

References: [1](Lide, Eleanor Lide David Alston Lide and Grace Eileen Lide David Austell Whitcomb Kate Elizabeth Whitcomb, 2003)[133], [2](Bell, 1973)[134], [3](Atkins, 2010)[135].

Equal amount of all the acids were used in the experiments. Various concentrations of the ethanol-water mixture were used. The ethanol-water mixture was prepared by diluting 92.5 % ethanol with water so that the final concentration of ethanol was from 9.0 to 89 %. Additionally, 99 % ethanol was used to study the effect in the highly concentrated environment. After adding 4 mL of 37 % HCl in the 99 % ethanol, the ethanol concentration was ~ 96 %. Hydrolysis in water without ethanol was carried out with the same, approximately 4.7, and 12.3 times higher HCl amounts.

3.2.2 Paper II: Synthesis of zwitterionic cellulose beads

The pristine cellulose beads were prepared as descrided elsewhere (Trygg et al.2013) with 10 % H_2SO_4 as coagulating system. A 5 % concentration of pretreated Enoalfa dissolving cellulose pulp with viscosity 124 ml/g was dissolved in 7 % NaOH 12 % urea-water system at -6 °C. The clear viscous solution obtained was dropped via spin drop atomizer into the coagulating bath. Spherical cellulose beads of average diameter between 250 µm and 4 mm were obtained. The wet beads were washed under running tap water until neutral pH achieved. The beads were further washed and stored in deionized water. The cellulose beads were oxidized by TEMPO-mediated oxidation reaction. Initially, the beads were immersed in 50 mM monosodium dihydrogen phosphate dihydrate ($NaH_2PO_4 \cdot 2H_2O$) buffer with maintained pH 4.6 overnight.

Table 3. Reagents dosage in (mmol/g) in different series of oxidation experiments.

OX series	OX-1	OX-2	OX-3	OX-4
$NaClO_2$	1. 5	3. 1	7. 4	12. 3
NaClO	0. 6	0. 6	0. 6	0. 6
TEMPO	0. 2	0. 2	0. 2	0. 2
HC series	HC-1	HC-2	HC-3	HC-4
$NaClO_2$	7. 4	7. 4	7. 4	7. 4
NaClO	0. 6	1. 2	1. 9	2. 5
TEMPO	0. 2	0. 2	0. 2	0. 2
TM series	TM-1	TM-2	TM-3	TM-4
$NaClO_2$	7. 4	7. 4	7. 4	7. 4
NaClO	0. 6	0. 6	0. 6	0. 6
TEMPO	0. 1	0. 2	0. 3	0. 4

To study the effect of reagents $NaClO_2$, NaClO and the catalyst TEMPO, three major sets of pristine cellulose beads were prepared and named as OX, HC and TM respectively. Further to study the effect of varying molar ratio of the reagents on the final carboxyl (COOH) and carbonyl (C=O) content in the oxidized beads, four subsets of each major set were prepared. The names of each set, subset and variation of the molar ratio of the reagents are described in (Table 3). The oxidation reaction was as follows- 10 g pristine cellulose beads (with 90 % moisture content) were equilibrated in sodium

dihydrogen phosphate dihydrate buffer. To the reaction mass added $NaClO_2$ followed by the TEMPO catalyst. Further NaClO was added dropwise in 15 mins. The reaction vessel was heated at 60 °C for 5 h with slightly open caps to release the chlorine gas evolved during the reaction. The reaction mass was cooled to room temperature and pH of the reaction was measured. The oxidized beads were continuously washed with distilled water until the conductivity measure reached below 10 µS/cm. The beads were stored in deionized water. The oxidized beads were further reacted with the Girard's reagent T to make the beads zwitterionic in nature. In a conical flask 1.0 g wet oxidized beads (OX1 and OX3) were equilibrated in 15 mL acetate buffer for 2h followed by the addition of Girard's reagent T (6.0 mmol/g). The reaction was heated at 60 °C for 1 h. The product obtained was washed, stored in deionized water and named ZW-1 and ZW-3. The scheme of the reaction is elucidated in Figure 7.

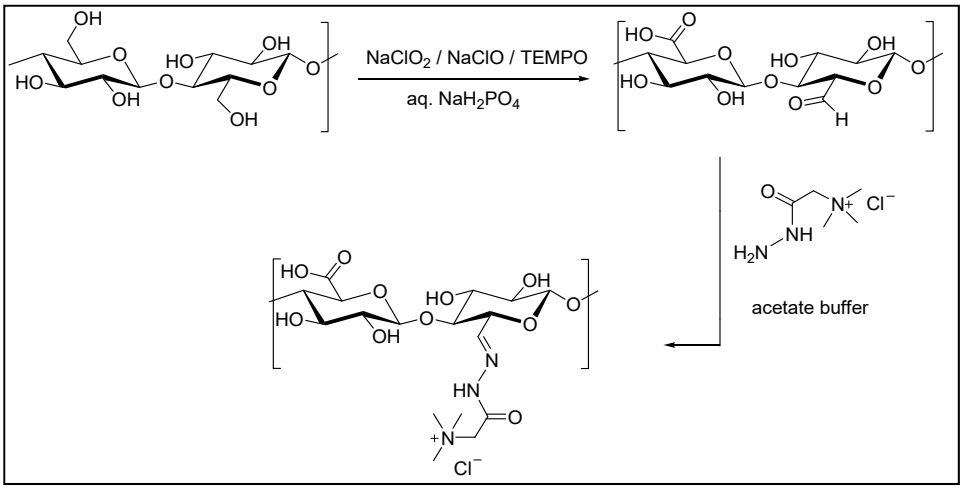

Figure 7. Schematic representation of oxidation and hydrazide coupling reaction performed on cellulose beads.

3.2.3 Paper III: Synthesis of sodium cellulose ethyl sulfonate (CES) and supramolecular design of anionic hydrogel beads

The reaction was set up in a 250 mL round bottom flask. Previously air-dried 8.1 g spruce sulphite pulp with DP_{Cuoxam} 450 was added in the 100mL 2propanol. To the reaction mass with continuous stirring, added a solution of 3.0 g sodium hydroxide and 3.2 g sodium vinyl sulfonate in 10 mins. Heated the reaction mixture at 80 °C for 1 h followed by the addition of an aqueous 10 mL solution of 3.2 g sodium vinyl sulfonate. After 3 h, further heating the reaction mass was cooled to room temperature and filtered. The product was neutralized with acetic acid and washed with 80 % 2-propanol to remove any byproducts generated during the reaction. The synthesized derivative had a degree of substitution of 0.48.

*CES and HyCellSolv Enoalfa cellulose pulp in 7 % NaOH-12 % urea-water solvent system were added in following ratios *0/100, *10/90, *30/70, 50/50, *70/30, *90/10 and *100/0 respectively to prepare blends. In a 30 mL glass vial, the polymers were added to the solvent system and stirred for 30 mins at room temperature. Then the blend was cooled to -6 ^{o}C for 1 h. The total polymer concentration in the blends was 5 % (w/w) and was stored at 0 ^{o}C prior to coagulation.

In order to select the appropriate coagulation system, following solvents were investigated: 2 M HCl, a mixture of 2 M HCl – ethanol (50:50), 50 % aqueous sodium sulfate and 2 M sulfuric acid. The 2 M sulfuric acid bath outperformed others. Therefore, all the hydrogel beads were coagulated in the 2 M sulfuric acid system. Briefly, the selected blend was filled in a 20 mL syringe and dropped through the needle with diameter 0.4 mm. The distance between the needle tip and the coagulating bath was 2 cm. The hydrogel beads were kept in the coagulation bath for 2 h to attain the final contour and washed with water until neutral pH achieved. The beads were stored in deionized water. Image J software is a Java-based image processing program which was used to analyse and study the shape and size of the beads.

3.2.4 Paper IV: Design of chitosan-cellulose hydrogel beads and cytocompatibility evaluation

The HyCellSolv treated cellulose pulp with DPυ 170 and chitosan with a degree of deacetylation (DDA) $\geq$ 75 % was added in the 7 % NaOH-12 % Urea – 81 % water solvent system and stirred at room temperature for 1h. The mixture obtained was cooled to – 13 ^{o}C for 1h and extruded in the form of beads via syringe with 0.8 mm needle diameter. Three different coagulating mediums used were 2 M acetic acid, 2 M hydrochloric acid and 2 M sulfuric acid. After 2 h, the hydrogel beads were washed with water until neutral pH was achieved and stored in deionized water.

Cytocompatibility analysis of chitosan-cellulose hydrogel beads with MDA-MB-231 (Human breast adenocarcinoma) cells

The cytocompatibility studies were performed in a humidified environment with 5 % CO_2 environment at 37 ^{o}C as per standard conditions. The DMEM supplemented with 10 % FBS, 2mM L-glutamine, and 1 % penicillin-streptomycin (v/v) was used as culture medium for the MDA-MB-231 cells (Human breast adenocarcinoma). The preselected hydrogel beads 0A, 70A, 0B, 70B and 0C, 70C were equilibrated in the culture medium in 96 well plates. The cells were added to the beads and the reaction was incubated for 48 h to evaluate the attachment and proliferation. After 48h, 10µL cell proliferation reagent WST-1 (Roche Diagnostics, Germany) was added to the respective wells. The plate was again incubated for 3 h at 37 °C, 5 % CO_2. After incubation, Tecan Ultra microplate reader (MTX Lab Systems, Inc.)

measured the absorbance at 430 nm. The measured absorbance was correlated with the number of viable cells. 10 % DMSO was used as positive control and cells were grown in the culture media without cellulose beads as a negative control.

Cytocompatibility analysis of Chitosan-cellulose beads coagulated in 2M acetic acid with Osteoblast cells

The osteoblast adhesion and proliferation studies were performed with 0A, 50A and 70A hydrogel beads previously soaked in MilliQ water. A set of 3 beads from each sample were sterilised and soaked in 1 mL cell culture medium the Advanced DMEM with 5 wt.% FBS for 30 minutes. In P96 well microtiter plate, Human bone osteoblasts (ATCC CRL-11372) were seeded at a concentration of 10.000 cells/well. The hydrogel beads samples were added in four repetitions to the cell wells after 24h incubation. The samples were used as prepared with the dilutions 1:2, 1:4, and 1:8 in Advanced DMEM with 5 % FBS. After 24h incubation under standard conditions, the biocompatibility/cytotoxicity was assessed using the MTT assay (Sigma-Aldrich, Germany). The cell viability was measured via the reduction reaction of tetrazolium salt MTT (3(4,5-dimethyl thiazolyl-2)-2,5-diphenyltetrazolium bromide) by measuring the absorbance at 570 nm using (Varioskan, Thermo Fisher Scientific Inc., Germany).

4. Analytical methods

4.1 Intrinsic Viscosity – Paper I, II, III and IV

Intrinsic viscosities of the pulps was measured to determine the degree of polymerization of studied pulps before and after the treatments. The standard ISO/FDIS5351:2009 was used and the average degree of polymerization was calculated from the formula $DP^{0.905} = 0.75 \times [\eta]$ (ml/g)[136]. Previously freeze-dried samples were weighed and dissolved in 0.5 M cupriethylenediamine (CED). The viscosities of the obtained solutions was measured via capillary viscometers. Standard operating conditions of maintained during all measurements. The capillary temperature was maintained at 25.0±0.1 °C. The limiting viscosity number also did not exceed more than 2 %.

4.2 Size Exclusion Chromatography (SEC) – Paper I

The molar mass distribution was measured with JASCO SEC system equipped with a degasser DG 980-50, pump 980, UV detector 975 working at k=254 nm, refractive index detector 930, columns Suprema1000+ and Suprema 100 from Kromatek, Great Dunmow, Essex, UK, with eluent flow rate of 1.000 mL min−1. Samples were dissolved in DMAc/LiCl solvent system and pullulan was used as a standard reference. The samples measured were dissolving grade Domsjö and HCS Domsjö pulps treated for of 0.5, 2 and 5 h, and with formic and nitric acids (2 h at 75 °C).

4.3 Carbohydrate analysis – Paper I

30 mg freeze-dried samples pulp samples were hydrolyzed with 300 µl 72 % sulfuric acid for 1h at 30 °C. The hydrolyzed samples were further diluted with 8.34 mL of deionized water. The samples were steam hydrolyzed in an autoclave for 1 h at 125 °C. 500µl clear hydrolysate was pipetted out and neutralized with ~ 50mM $Ba(OH)_2$. The neutralization process was performed with the utmost care so that the pH did not exceed 8.5. Sorbitol standard was used as an internal reference. The arabinose, galactose, glucose (Glu), rhamnose, xylose (Xyl), and mannose (Man) concentrations were analysed with a high-performance liquid chromatography (HPLC) Dionex ICS 5000 system equipped with a pulsed amperometric detector (PAD), single pump, dual piston and online degasser. Potassium hydroxide (KOH) was used as an eluent. The analytical column was a CarboPac PA20 (3x150 mm) with an attached CarboPac PA20 guard column (3x50 mm). The eluent flow rate was 0.35 mL min^{-1}. Chromeleon 7.0 software, purchased from ThermoScientific was used for data processing and analysis.

4.4 Anionic group determination – Paper I

The anionic group content of pulps was measured by methylene blue (MB) adsorption isotherms [137]. Sorption experiments were performed at 25 °C and concentrations of free MB were determined with UV-Vis spectrophotometer (Shimadzu UV-2600 Japan).

4.5 Conductometric titrations and pH measurements – Paper II

Conductivity titrations were performed to determine the carboxylic content in the oxidized beads. Mettler Toledo Seven Excellence pH/Conductometer equipped with InLab Expert ProISM electrode and InLab 738 ISM conductometric sensor was used for pH and conductometric measurements. SCAN-CM 65:02 standard protocol was used with slight modification for conductometric titrations. Wet beads were crushed and the slurry obtained was titrated. The dry content of the samples after titration was determined by freeze-drying the samples and weighing.

4.6 Elemental analysis (EA) – Paper II, IV

In paper II, the nitrogen content in the samples was measured by the Organic elemental analyzer, Flash 2000, from Thermoscientific. Crushed air dried bead samples were used for the analysis. The nitrogen content measured was used to quantify quaternary ammonium hydrazide groups in the zwitterionic beads. Methionine was used as a calibration standard and sulphanilamide as check standard. Standards were purchased from Elemental Microanalysis Limited. Air dried beads were used for the analysis.

In Paper IV, A VARIO EL III CHNS analyzer (Elementary Analysen system GmbH) was used for elemental analysis of the lyophilized chitosan cellulose hydrogel beads according to standardized procedures. The chlorine content was determined subsequently by combustion of the organic samples and potentiometric titration with $AgNO_3$ using a chloride-sensitive electrode.

4.7 Scanning Electron Microscopy-Energy Dispersive X-ray Analysis (SEM-EDX) – Paper III

Surface-core morphology and sulphur weight percentage analysis of beads were performed with an LEO Gemini 1530 scanning electron microscope. The Thermo Scientific Ultra Silicon Drift Detector (SDD) equipped with secondary electron backscattered electron and in-lens detector. Surface dried hydrogel beads were frozen in liquid nitrogen and freeze-dried under vacuum to maintain the pore structure. The dried beads were cut into cross sections coated with carbon and analyzed. The magnification of image corresponds to a Polaroid 545 print with the image size of 8.9 × 11.4 cm.

4.8 Attenuated Total Reflectance-Fourier Transform Infrared (ATR-FTIR) and Raman spectroscopy – Paper II, III and IV

The functional group confirmation in the beads was performed by Nicolet iS 50 FT-IR spectrometers with Raman module from Thermo Scientific. FT-IR spectra were collected using Tungsten-halogen source and DLaTGS-KBr detector splitter set up with 4.00 cm-1 resolution and 128 scans. Raman spectra were collected using a diode laser (power-0.5 W). The detector was InGaAs with CaF_2 splitter; resolution 8.0 cm^{-1} and number of scans 1000. Dried samples were used for the analysis.

4.9 Solid state ^{13}C and ^{15}N NMR spectroscopy – Paper II and IV

The solid-state ^{13}C and ^{15}N NMR spectra of the crushed bead samples were recorded with 400 MHz Bruker AVANCE-III NMR spectrometer equipped with a 4 mm CP MAS probe; operating frequencies 399.75 MHz (1H), 100.52 MHz (^{13}C) and 40.51 MHz (^{15}N). The spectra were recorded at the spinning rate of 7 and 5 kHz and a contact time of 5 and 2 ms (^{13}C) and 3.5 ms (^{15}N).

4.10 Scanning Electron Microscopy (SEM) analysis – Paper I, II, III and IV

The morphological analysis of the samples was performed with LEO Gemini 1530 with a Thermo Scientific ultra Silicon Drift Detector (SDD). The samples were frozen under liquid nitrogen atmosphere and freeze-dried to maintain the pore structure.

4.11 Rheology Measurements – Paper II

The storage-loss moduli and viscosity of 5 % (w/w) polymeric blends in a solution of 7 % NaOH-12 % urea-water system at 10 ^{o}C and 25 $^{o}C \pm 0.1$ were measured by oscillatory and steady-state rheological experiments. Anton Paar Physica MCR 300 rotational rheometer with double gap cylinder module DG 26.7 with attached temperature controlling TEZ 150P thermostat possessing external water circulation. Each blend was stored at 0 ^{o}C (± 1) before measurements. The frequency was varied from 0.5 to 500 Hz for the oscillatory measurements and the steady shear rate was increased from 0.1 to 1000 s^{-1} for viscosity. The results were summarized by Rheo plus 32 software.

4.12 Water holding capacity (WHC) Paper II

The role of increasing sulfonate content on water holding capacity was determined by removing surface water from the hydrogel bead on filter paper. 20 wet beads prepared from each blend were weighed in triplicate sets and dried in an oven at 60 $^{o}C \pm 1$. The samples were cooled in a

desiccator until constant weight was achieved. The WHC in percentage was determined using the following equation.

$$\text{WHC}\ (\%) = (w - w_d)/w_d \times 100$$

Where w is the total weight of wet beads, and w_d is the total weight of dry beads.

4.13 ToF SIMS analysis- Paper I

Air dried samples were used for the analysis. Physical Electronics ToF–SIMS TRIFT II spectrometer with a $^{69}Ga^{+}$ primary ion beam was used for surface analysis. The raster size was 200 µm x 200 µm with a resolution of 256 x 256 pixels. The spectrometer was operated in the positive mode with 25 kV applied voltage and 600 pA aperture current.

4.14 X-Ray diffraction (XRD) analysis Paper IV

The XRD measurements of chitosan-cellulose dried bead samples were performed on a Bruker D8 Discover instrument (Bruker, Karlsruhe, Germany) with a Cu K_α X-ray source and an HI-STAR area detector. The incident angle was kept at 6°, while the detector angle (2θ) was 25°.

5. Results and Discussion

5.1 Controlled depolymerization of pulps

5.1.1 Effect of acids and ethanol on the degree of polymerization of pulps

The chemical pretreatment of the studied pulps, described in Table 4 was studied with different chosen acids based upon their pKa as mentioned in the Table 2 in the methods section 3.2.1. The impact of solvent used on the degree of polymerization of pulps provided an insight about the chemistry behind the controlled depolymerization.

Table 4. The studied pulps and their composition

Pulp	Supplier	Raw material - Pulp grade
Domsjo	Domsjö Fabriken	Spruce/Pine – Dissolving grade
Enoalfa	Stora Enso	Birch/Aspen- Dissolving grade
BNP (Botania Nordic Pine)	Metsa Fibre	Pine- Kraft
Euca	UPM-Kymmene	Eucalyptus - Kraft
Birch	UPM-Kymmene	Birch - Kraft

The pretreatment of Domsjö pulp under aqueous - hydrochloric acid conditions resulted in the reduction of DPυ values from 737 to 291 along with a decrease in cellulose content. An increased hydrochloric acid concentration of 4.7 and 12.3 times higher resulted in a notable decrease in DPυ values of 158 and 123 respectively. The addition of ethanol in the solvent system affected the DPυ reduction only after the 36 % ethanol concentration. A continuous decrease in DPυ from 36 % to 76 % ethanol concentration was observed. While after 76 % a sharp decrease in the values was observed as shown in (Figure 8a). The activity coeffiecint of hydrochloric acid increases with the addition of ethanol. At 76 % ethanol concentration in the pretreatement, liquor the activity coeffieicent value of hydrochloric acid is more than 5. Therefore the decrease in DPυ with increasing ethanol concentration was related to the competing reaction between ethanolysis-hydrolysis and the increased activity coefficient of the hydrochloric acid[138]. Further to study the effect of various pre-decided acids and their pKa on the DPυ of Domsjo pulp, HyCellSolv pretreatment was performed. The chosen acids were added into the ethanol-water systems same as used in the hydrochloric acid treatement with 89 % ethanol environment. The treatment with stronger acids (with pKa $\leq$ 0) for instance sulfuric or perchloroic acid resulted in DPυ between 177-258. While with weaker acids (with pKa $\geq$ 0), the DPυ was between 449-754 (Figure 8b).

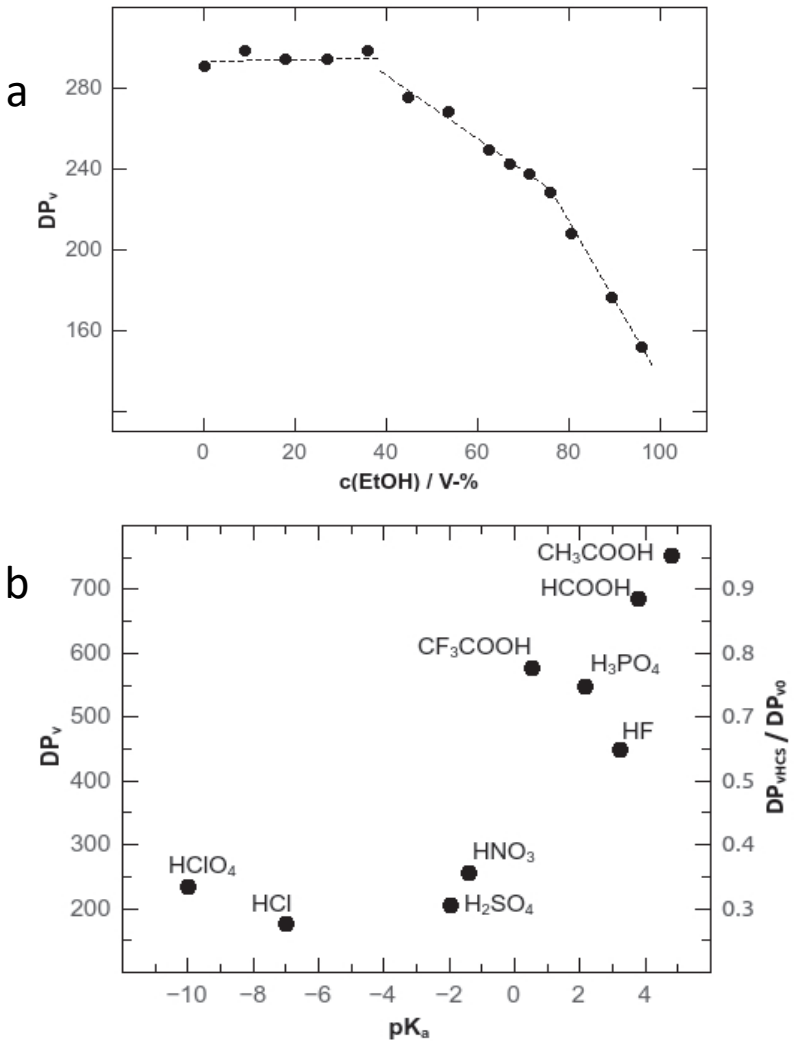

Figure 8. a) DPυ of HCS-Domsjö pulp with variying ethanol concentrations after HyCellSolv-treatment, b) DPυ of Domsjö-pulp after HyCellSolv treatment with different chosen acids. The Right y-axis shows the ratio between the measured DPυ HCS of HCS-Domsjö and initial $DP\upsilon_0$ of Domsjö-pulp

These results could be explained by the well-known fact that the LODP depends upon the concentration of the hydrogen ions generated from the acid[42,140].

The monosacchride composition analysis of hydrolysate of Domsjö pulp treated under various conditions showed that, pretreatment in water resulted in heavy loss of glucose content, thus resulting in relative increased concentrations of xylose and mannose. Addition of ethanol from 9.0 to 89 % had a positive impact on the loss of glucose as apparent in the (Figure 9).

Therefore, it can be concluded that, addition of ethanol results in degradation of cellulose into water insoluble units instead of water-soluble components.

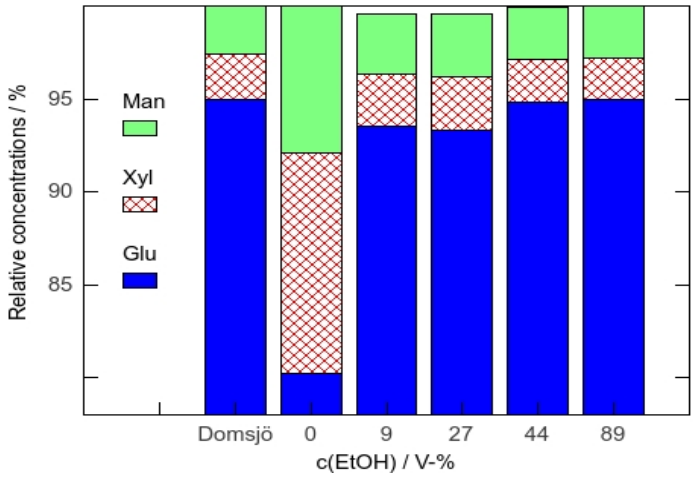

Figure 9. Relative monosaccharide concentrations of Domsjö pulp hydrolysate before and after HyCellSolv treatement with 0 - 89 % ethanol concentrations.

In the case of molar mass distribution, also a decreasing trend was observed with the increasing strength of the acids. The formic acid-treated pulp did not show much variation in the molar mass distribution from the untreated cellulose. While hydrochloric acid treatment displayed much-pronounced reduction in the molar mass distribution as shown in the (Figure 10).

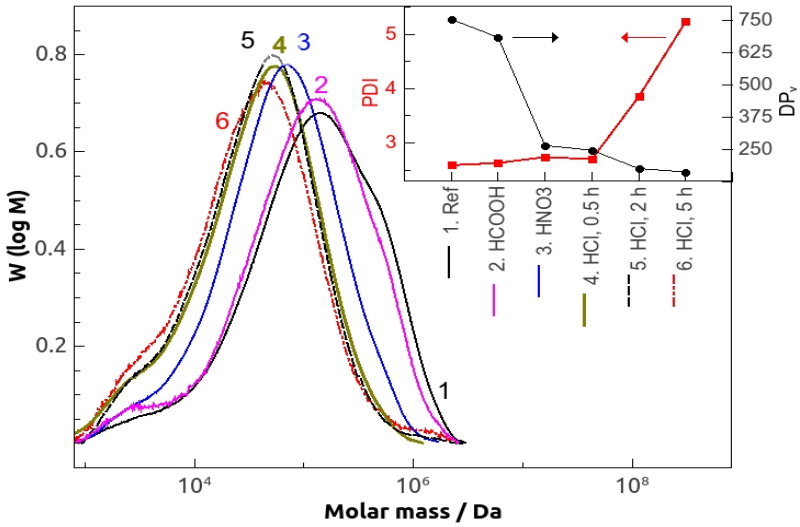

Figure 10. Molar mass distributions, polydispersity indices and DP*v* values of Domsjö-pulp before and after HyCellSolv-treatment with formic (2) nitric (3) acids for 2 h, and HCl for 0.5 (4), 2 (5) and 5 h (6).

This resulted in increased concentration of lower molar mass polymers with M*w* < 10^4 Da. It is known that the molar mass Mw < 10^4 Da are mainly composed of hemicelluloses. During the pretreatment, no degradation of hemicellulose was observed, therefore it is presumed that, the decrease in high Mw cellulose resulted in increased units with molar mass Mw < 10^4 Da.

The measured $DP\upsilon_o$ values of untreated and pretreated pulps showed that birch pulp has the highest $DP\upsilon_o$ amongst all pulps. After pretreatment, reduction in DPυ was observed in all the pulps (Table 5). The ratio of DPυ HCS/ $DP\upsilon_o$ of pulps showed that the pretreatment was mostly ineffective in case of Euca pulp. The charge of the pulps is mainly due to hemicelluloses and uronic acid. In case of dissolving grade pulps, not much difference in charge was observed after pretreatment. While in case of Kraft pulps the reduction in charge occurred due to a loss in hemicelluloses during the pretreatment process.

Table 5. DP**υ** and charge of pulps before and after HyCellSolv treatment and ratio of DP**υ** values.

Pulp	DPυ0	DPυ HCS	DPυ HCS/ DPυ0	Initial Charge (µmol/g)	Final Charge (µmol/g)
Domsjo	737	*291/183	0.248	39	*35/25
Enoalfa	652	159	0.244	53	42
BNP	1182	252	0.213	56	42
Euca	1238	252	0.204	75	46
Birch	1318	331	0.251	94	46

*without ethanol

5.1.2 Effect of pretreatment on the dissolution mechanism of pulps

The dissolution mechanism of pulps was studied in 0.2M CED solution and visualized via optical microscopy. A comparison between untreated and pretreated pulps showed that untreated pulps displayed ballooning behaviour, which is well obvious. While in the case of pretreated pulps, only Domsjo pulp dissolved via complete fragmentation. Other pulps showed uniform swelling behavior and some fragmentation (Figure 11 and Table 6).

The ballooning effect was not observed speciafically in any HCS treated pulp except in BNP pulp, where initial partial ballooning was observed. The Initial partial ballooning could be due to the high hemicellulose content and high DPυ. As we have already discussed, the stronger acid treatment led to a relatively lower DPυ than the milder acid treatment. A similar trend was also observed with the dissolution behaviour mechanism of the pulps. The HCS Domsjö pulp fibres dissolved via fragmentation after the treatment with strong mineral acids, whereas the fibres swelled uniformly and showed only some fragmentation with phosphoric acid.

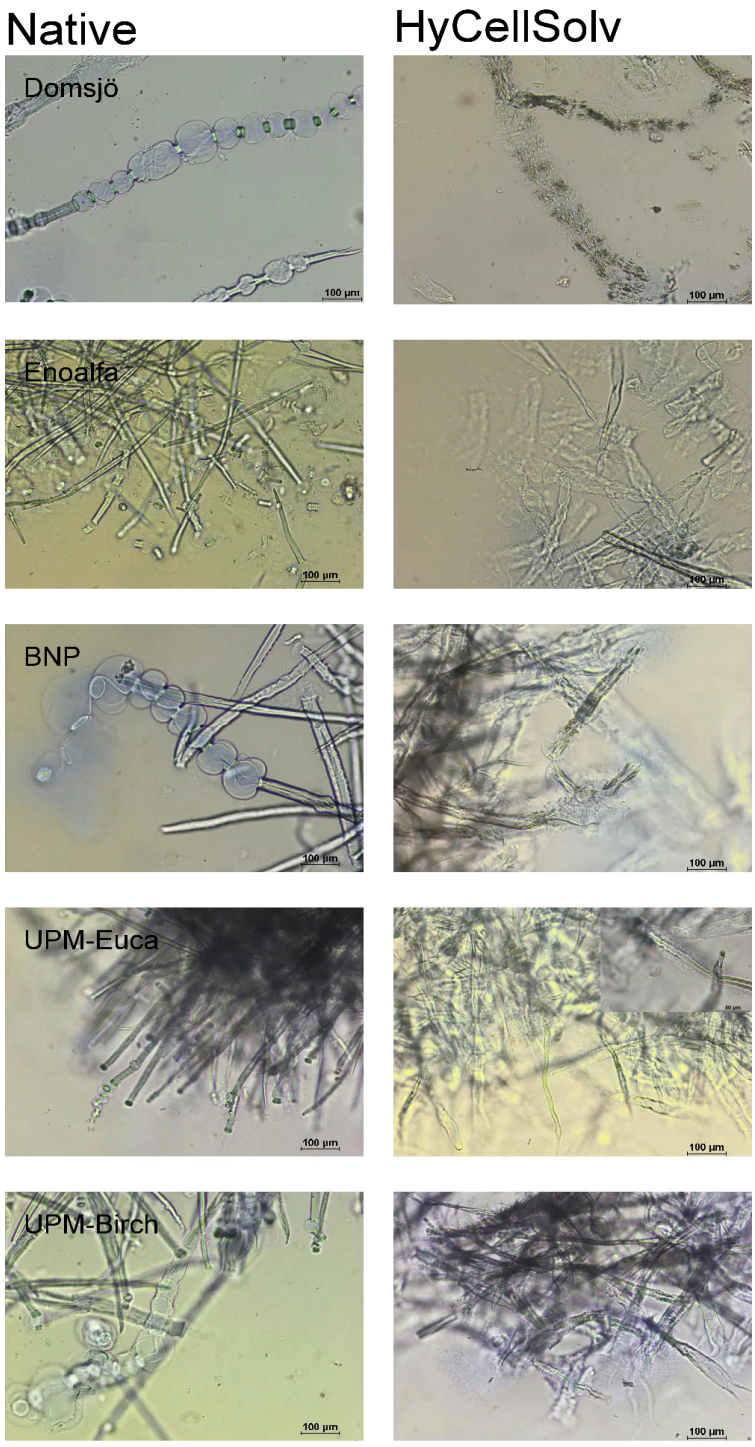

Figure 11. Domsjö, Enoalfa, BNP, UPM-Euca and UPM- Birch pulps. Untreated (left column) and HyCellSolv-treated (right column) in 0.2 M CED solution.

In the case of hydrofluoric acid fibres swelled uniformly before dissolution and only ballooning was observed with formic acid. The ballooning behavior in case of formic acid could be related to the higher p*Ka* value (3.75) of the acid, as compared to the phosphoric acid (p*Ka* 2.16) and hydrofluoric acid (p*Ka* 3.2).

Table 6. Dissolution mechanism of various pulps under different conditions in 0.2M CED.

HCS Pulp	Acid pKa & HCS Domsjo	Ethanol concentration (%)
Domsjo - **F**	Hydrochloric (-7)- **F**	28 to 96 - **F**
Enoalfa- **U**	Sulphuric (-2)- **F**	19 – **U/F**
BNP - **U**	Trifluoroacetic (0.52)- **B**	0-9 - **U**
Euca - **U**	Phosphoric (2.16) -**U/F**	
Birch - **U**	Hydrofluoric (3.2)- **U**	
	Formic (3.75)- **B**	

Dissolution mechanism: B–dissolution via ballooning, U–uniform swelling, F–fragmenting

In order to evaluate the role of ethanol concentration in the pretreatment liquor on the dissolution mechanism of HCS- Domsjö pulp, following observations were made as shown in (Table 6). The pulp treated with low ethanol concentrations i.e., 0-9 % showed uniform swelling of the fibres before dissolution while after 19 %, uniform swelling and fragmentation was observed. While above 28 % ethanol concentration, only fragmentation was visible. Therefore, we can conclude that, the ethanol concentration also plays a significant role in deciding the dissolution mechanism of the HCS-Domsjö pulp fibres along with the acid pKa.

Therefore, it is possible to control the depolymerisation of the pulps by choosing the appropriate acid, ethanol concentration and time of pretreatment. The process also results in minimum loss of cellulose into soluble products, thus leading to enhanced recovery of the final pretreated cellulose.

5.2 Effect of introducing zwitterionic moieties in the cellulose beads

5.2.1 Determination of carboxylic and carbonyl content in cellulose beads and introduction of quaternary ammonium group in oxidized beads.

The pristine cellulose beads were designed by dispersion, dissolution of Enoalfa HyCellSolv pulp in 7 % NaOH-12 % Urea-81 % water followed by

coagulation in 2 M sulfuric acid. The beads were further functionalized by introducing carboxylic and trimethyl ammonium hydrazine moieties. The cellulose beads were oxidized by $NaClO_2$/NaClO/TEMPO system mediated oxidation reaction. Although the most obvious oxidation reaction is the generation of carboxylic groups, along with that, some carbonyl groups are also present[141]. The carboxylic content in the beads was measured with conductometric titrations and carbonyl content by oximation followed by nitrogen element analysis. The beads with a variation of $NaClO_2$ (OX series) in the reaction medium showed an increasing trend of COOH/C=O content from 0.56/0.33 (OX-1), 0.62/0.38 (OX-2), 0.98/0.55 (OX-3) up to 1.35/0.79 mmol/g (OX-4) (Figure 12a). The reason of increased anionic charge and the carbonyl content could be explained by the fact that the $NaClO_2$ is the primary oxidant in the reaction medium. An increase in the molar ratio of $NaClO_2$ leads to increased oxidation[142–144] While a variation of NaClO (HC series), the ratio of COOH/C=O was 1.08/0.34 (HC-1), 1.4/0.40 (HC-2), 1.18/0.29 (HC-3) up to 1.23/0.41 mmol/g (HC-4) (Figure 12b). All the samples showed a regular increasing trend in anionic charge and carbonyl content except the HC-3 where the carbonyl content was low as compared to others. The increasing molar ratio of TEMPO catalyst (TM series), from 0.1 to 0.2 mmol/g lead to considerably higher carboxylic content than 0.3 and 0.4 mmol/g and a linear rise in carbonyl content (Figure 12c). Therefore, it is possible to tune the ratio of carboxylic versus carbonyl content in the cellulose beads by varying the molar ratio of the reagents. Also, the generation of carboxylic and carbonyl content together in cellulose beads provides an opportunity for introducing new functionalities into the beads.

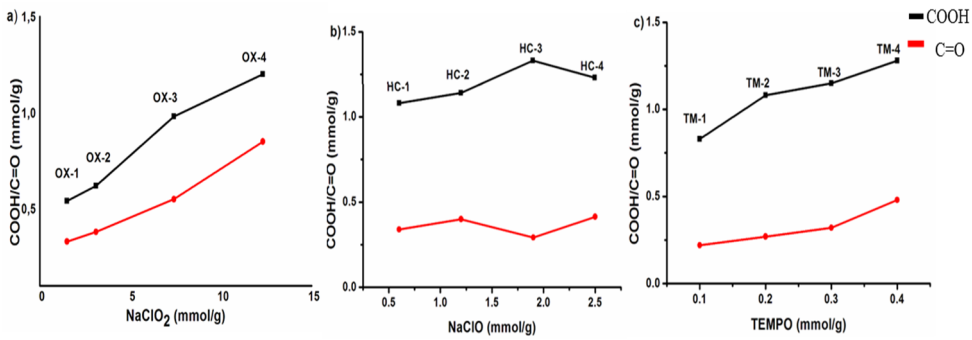

Figure 12. Effect of varying molar ratio of reagents on COOH and C=O contents: a) NaClO2, b) NaClO, c) TEMPO

A reaction between a hydrazide and carbonyl group of aldehydes results in the formation of stable hydrazone [145–148]. It is similar to a coupling reaction between an aldehyde and a primary amine which results in the formation of Schiff's base in weak acidic environment [149]. Utilising the approach of coupling chemistry between carbonyl and hydrzide, the oxidized beads

samples OX-1 and OX-3 were reacted with Girard's reagent T, thus transforming them into zwitterionic (ZW) beads. The measured quaternary ammonium group content in the ZW-1 and ZW3 was 0.16 and 0.39 mmol/g respectively. Therefore, up to 50–60 % carbonyl groups reacted with the hydrazide reagent confirming the formation of zwitterionic beads under heterogeneous environment.

5.2.2 Functionalization confirmation and morphological evaluation of zwitterionic beads

A detailed spectroscopic analysis of the reference, oxidized and zwitterionic cellulose beads was performed by ATR-FTIR, Raman and ^{13}C NMR techniques. In the ATR-FTIR spectrum, a prominent peak in the range of 1600–1700 cm^{-1} due to the out of phase stretching vibrations and in phase stretching at 1414 cm^{-1} due to carboxylate (COO-) group was observed in OX-3 and ZW-3 beads in comparison to the reference cellulose bead (Figure 13a). In ZW-3 a new peak in the region of 1680 cm^{-1} corresponding to the presence of carbonyl group of amide bond CONH in the formed hydrazone linkage. The imine bond at 1567 cm^{-1} was considered to be overlapping with the C=O band of COO- group [150]. A distinct peak at 1473 cm^{-1} shows the presence of quaternary ammonium group. Similarly in Raman spectrum also at 3010–3022 cm^{-1} new peaks are observed due to the $CH_2–N^+(CH_3)_3$ moiety. Another peak due to CH(C=O) stretching vibrations at 2925 cm^{-1} are visible (Figure 13b).

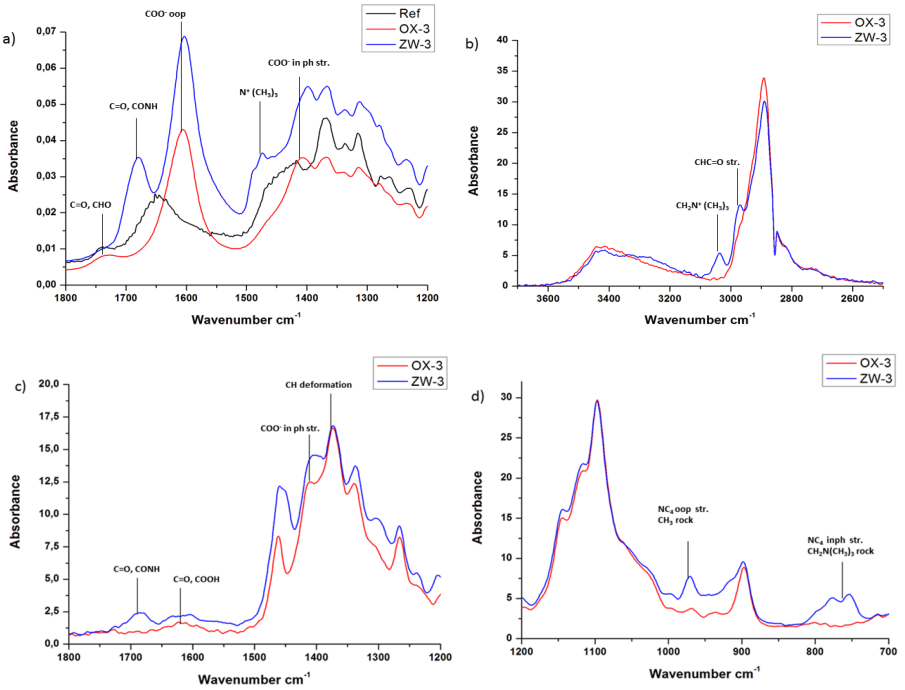

Figure 13. a) ATR-FTIR spectra of cellulose (ref), oxidized (OX3), and zwitterionic (ZW3) beads b)-d) Raman spectra of oxidized (OX3), and zwitterionic(ZW3) beads.

Weak signals due to carboxylate COO- and amide functional groups are also present at 1700–1500 cm^{-1} (Figure 13c). Peaks at 955 cm^{-1} and 720 cm^{-1} regions corresponding to NC_4 out of phase stretching vibration, CH_3 rocking and NC_4 in phase stretching vibrations are also visible confirming the presence of carboxylic acid groups and quaternary ammonium groups after oxidation and hydrazide coupling in cellulose beads under heterogeneous conditions (Figure 13d).

Further investigation of cellulose, oxidized cellulose and zwitterionic beads by Solid-state ^{13}C NMR spectroscopic analysis was performed to confirm the introduction of carbonyl, carboxylic and quaternary ammonium functional groups as shown in (Figure 14). In the cellulose beads reference spectrum characteristic signals due to C1 (107 ppm), C4 (89 ppm), C2, C3, C5 (70–80 ppm) and C6 (64 ppm) were present. The ^{13}C NMR spectra of the oxidized cellulose beads also showed the characteristic signal of carboxylic acid functionality at 176 ppm [144]. While in the spectrum of zwitterionic beads a signal at 56 ppm due to the carbon atoms in the N-trimethylated group was present [151]. Although the aldehyde group could not be explicitly observed as they probably occur in hydrated or hemiacetal form. These results confirm the formation of zwitterionic cellulose beads via reaction between the aldehyde groups of the oxidized cellulose beads and the hydrazide reagent.

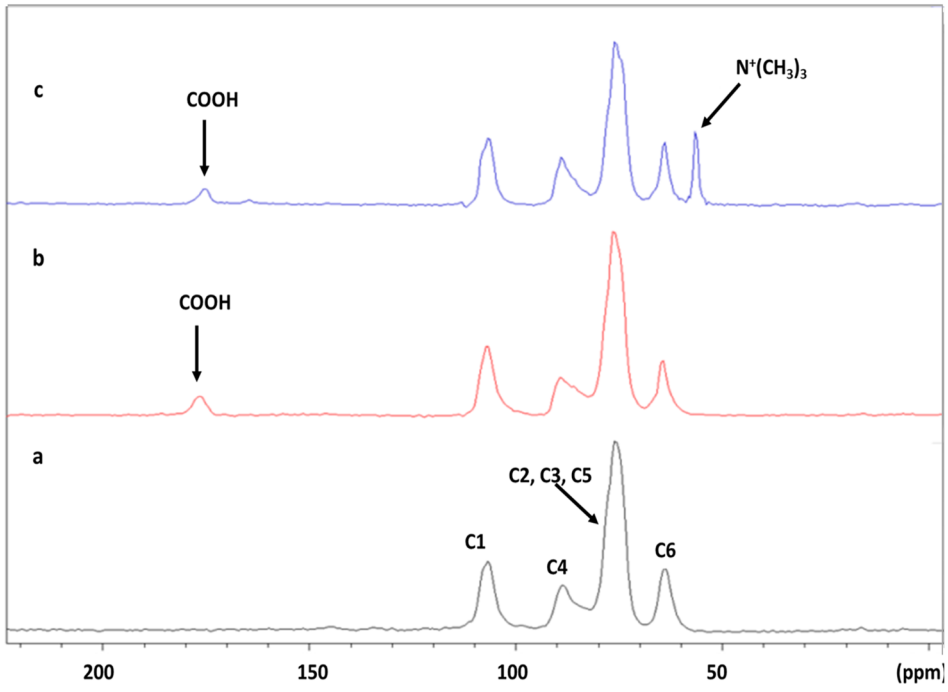

Figure 14. CPMAS ^{13}C solid state NMR spectra of a) Reference bead, b) Oxidized bead (OX-4) c) Zwitterionic bead (ZW-4)

The effect of functionalization of cellulose beads into zwitterionic also resulted in changes in the moprphology and ultrastrucure of the beads. The SEM analysis showed variation in the pore structure between reference and the zwitterionic beads. In case of reference beads, a more interconnected inner structure was observed while zwitterionic beads displayed a relatively macroporous structure (Figure 15). The generation of macroporous internal structure in the zwitterionic beads was related to the increased hydrophilicity of beads in relation to the generation of ionic moieties.

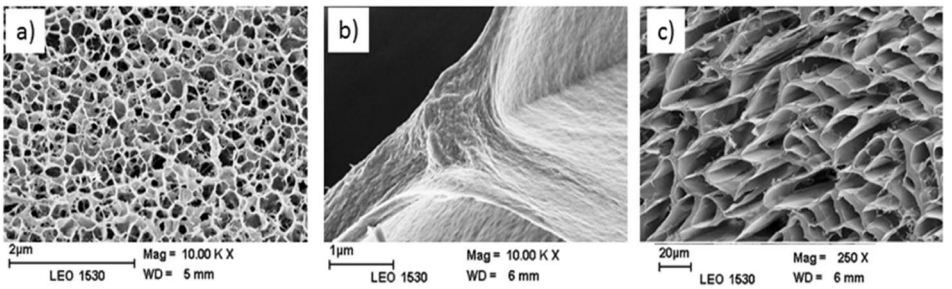

Figure 15. Cross sections of reference (a) and zwitterionic (b, c) of cellulose beads

5.3 Effect of blending sodium cellulose ethyl sulfonate (CES) on the supramolecular design of cellulose hydrogel beads

5.3.1 Rheological Behavior of Blends

The rheological behaviour of the polymer blends plays a decisive role in designing a hydrogel bead and their physical properties such as stability, shape and porosity. The rheology of 5 % (w/w) polymer blends solutions was studied to understand the effect of increasing CES content on viscosity and storage and loss moduli with varying shear rate in blends.

In 7 % NaOH– 12 % urea-water solvent system, 5 % CES and Enoalfa HCS pulp showed viscoelastic behaviour with frequency and temperature dependent storage (G′) and loss moduli (G″) (Figure 16a). The temperature dependent results showed that at 10 °C, the storage modulus of CES was higher than at 25 °C. This is a typical behavior of charged polymers having increased dispersibility in aqueous systems. The Enoalfa HCS pulp showed no characteristic temperature-dependent variation as the dissolving pulp have low surface charge and less dispersibility in the aqueous solutions. Increasing frequencies resulted in a continuous increase in (G′) and (G″) (Figure 16 a). Therefore, viscous behaviour was predominant over the elastic in the case of both the polymer solutions. A levelling off behaviour for (G′) was observed in case of Enoalfa HCS pulp only in the frequency

range 10-100 Hz. It could be due to the loss of elasticity due to entanglement or coiling of the polymer with the increasing frequency[152].

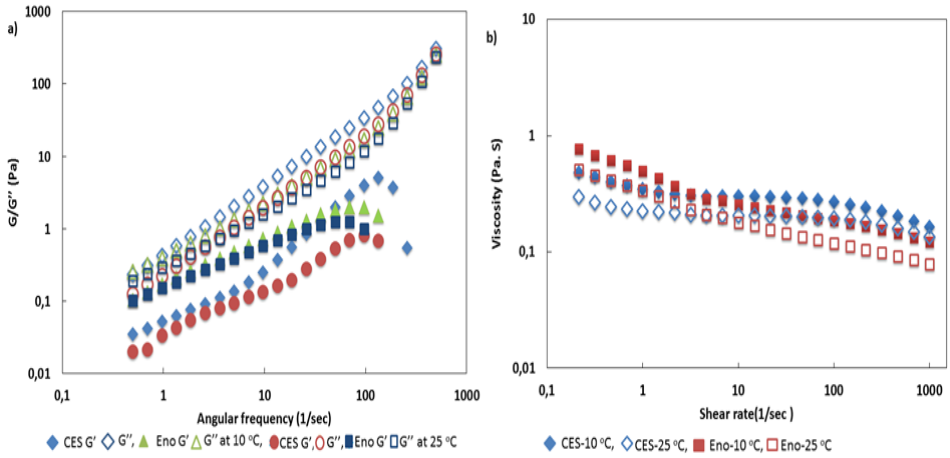

Figure 16. a) Change in the storage (G′) and loss (G″) moduli with increasing angular frequency (Hz) and b) Viscosity vs. shear rate at 10 °C and 25 °C of CES and HCS -Enoalfa.

It was predicted that the solvent system was not interacting with the polymeric material due to the low surface charge. Thus, the dissolved polymers are less stretched but more coiled in the solvent. Therefore, the elastic behaviour of the coiled structure cannot increase above a certain frequency range. While in the case of CES polymer solution a continuous increase in the elastic modulus (G') was observed, which could be explained by the charge-driven interaction between CES and solvent, leading to a more stretched out or swollen polymer structure.

The steady shear rate dependent viscosity measurements showed that as compared to 5% Enoalfa pulp solution, the CES solution had a lower viscosity at both the temperatures at the low shear rate (Figure 16b). It could be due to the higher solubility, ionic nature and weak hydrogen bonding of CES. A non-Newtonian behaviour was observed in case of both the polymer solutions. Although CES displayed a plateau in the range of 10–100 s^{-1}, further decrease in viscosity was observed above 100 s^{-1} shear rate. At 25 ^{o}C, both the polymer solutions displayed higher viscosity than at 10 ^{o}C. The oscillatory and shear rheology of the blends were investigated to get an insight into the flow and stability properties of polymeric blends of CES and Enoalfa pulp. As it is a well-known fact that to prepare stable blends, polymeric associations or repulsions and polymer-solvent interactions play a very critical role. The predominant interactions present in polymeric blends are van der Waals forces, hydrogen bonding, and ionic interactions[153].

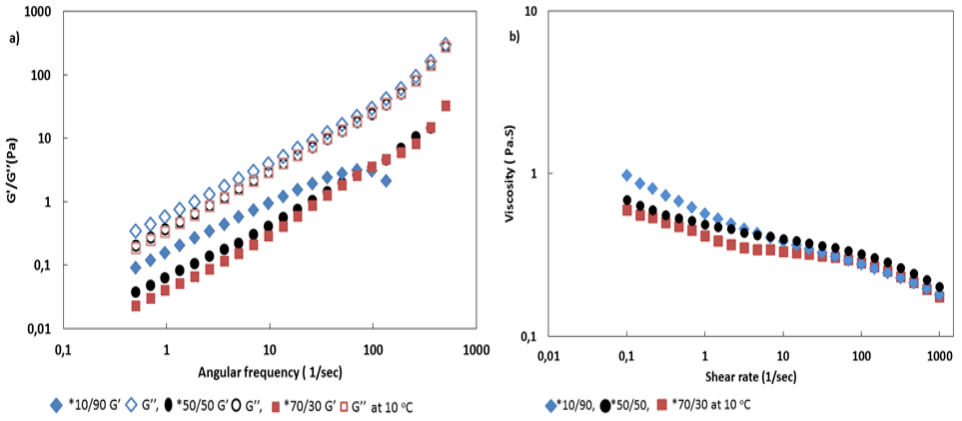

Figure 17. a) Storage (G′) and loss (G″) moduli and b) Viscosity vs. shear rate of various blends of CES:Enoalfa at 10 °C.

At 10 °C the *10/90 (CES/Enoalfa) blend (G′) showed comparatively higher values than the *50/50 and *70/30 blends as shown in (Figure 17a). Due to the high content of Enoalfa in case of *10/90 blend, a plateau of (G′) was visible at the increasing frequency from 50–100 Hz. It was observed in that the loss modulus (G″) was always greater than the storage (G′) for each blend at 10 °C. The viscosity results of blends displayed that at a low shear rate the *10/90 solution had a slightly higher viscosity closer to one (Pa.s) in comparison to *50/50 and *70/30 blends (Figure 17b), which could be due to the higher intermolecular associations in polymeric subunits. No such difference was observed amongst the blends at a high shear rate, as shear thinning was predominant due to more intramolecular interactions and elongation of polymeric chains. The lowering of viscosity could also be related to the increased CES concentration thus leading to the increased overall surface charge of the solutions which in turn resulted in enhanced electrostatic repulsions, disentanglement and loosening of the network structure[152,154]. Hence, the rheological studies showed that an increase in ionic polymer concentration in the blends leads to a reduction in viscosity and storage modulus (G′) at a low shear rate and low angular frequency respectively.

5.3.2 Role of CES Polymer on the Properties of Hydrogel Beads

The viscosity studies showed that there is a variation in the solution properties of pristine Enoalfa cellulose solution, CES solution and varying mixture solutions of both the polymers. Thus, the role of CES concentration on the designed hydrogel beads was further investigated to understand the underlying mechanism. In case of alkali cellulose coagulation in the acidic medium, ion exchange between OH^- and H^+ ions occurs, which results in phase separation of the dissolved cellulose polymer[155]. The coagulation of

various polymer concentrations of blends ranging from *10/90 to *90/10 in the 2M sulfuric acid system resulted in the formation of entities with variable contour. The shape of the beads varied from spherical to the flattened discs like with increasing CES concentration in the blends (Figure 18a). The 100% CES also precipitated out slightly, which could be due to the ion exchange thus protonating the sulfonate ions to sulphonic acid. Therefore, the role of Enoalfa polymer in the blends is crucial to define the shape and stability of the hydrogel beads.

The average size of the beads was extracted from the processed binary images. The results showed that the average size of the *0/100 beads was 6mm, which increased drastically to 11.7mm for the beads prepared form *70/30 polymer concentration (Figure 18b). The increase in the average surface area is directly correlated to the flattening of the beads with increasing polymer concentration. These observations could be related to the lowering of the measured viscosity of the blends with increasing CES polymer concentration in the blends. For instance, the measured viscosity of *0/100 and *70/30 beads at the shear rate 0.1 s^{-1} are approximately 0.9 and 0.7 Pa.S respectively.

The measured water holding capacity of the beads also varied with the increasing CES polymer concentration in the blends. The *0/100 beads showed 93.7 % water holding capacity, which increased up to 97 % in case of *50/50 beads. The water holding capacity is directly correlated to the rising sulfonate content which consequently to the surface charge of the beads, resulting in favourably absorbing a higher amount of water. The measured sulphur content in the beads showed that the beads retained almost the same CES polymer concertation in the beads produced from *50/50 blend after coagulation and washing as per the initial content of the added CES in the polymer blend. The sulphur content of CES was 8.75 % by weight and in *10/90, *30/70 and *50/50 beads the sulphur content was 1.1 %, 2.8 % and 4.3 % ($\pm$0,25), respectively. The beads prepared from *10/90 up to *50/50 ratio were stable at pH 6, while notable scaling was observed in the beads with higher CES concentration. This could be due to increased CES concentration, which in turn resulted in increased anionic charge content in the beads. Consequently, the increased ionic repulsion interactions due to ionized sulfonate groups led to destabilized structures at neutral pH[156].

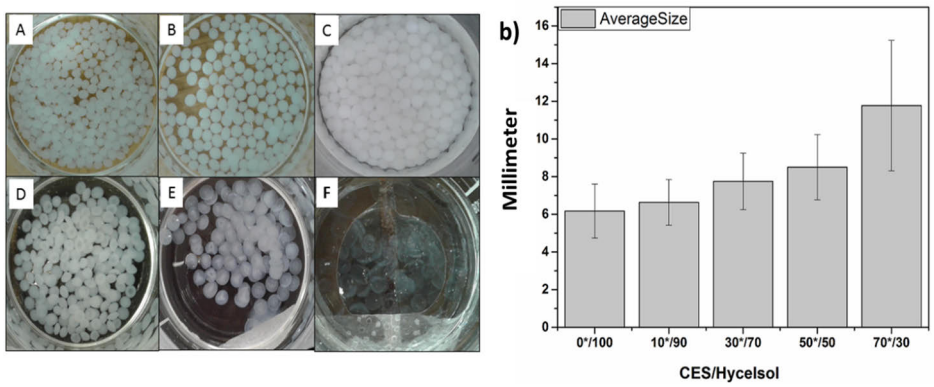

Figure 18. (a) Cellulose hydrogel beads with increasing *cellulose ethyl sulfonate concentration: A) *10/90, B) *30/70, C) *50/50, D) *70/30, E) *90/10, F) *100/0. (b) Average increase in the size of beads.

5.3.3 Confirmation of CES retention and morphology of the hydrogel beads

The retention of CES polymer in the hydrogel beads was further confirmed by the ATR-FTIR and Raman spectrometry. The spectral range from 1600–500 cm^{-1}, provided significant information about the sulfonate groups in the beads. In FTIR spectrum the region 1100–1400 cm^{-1}, displayed distinct peaks due to SO_2 in-phase, out-of-phase and SO_3 in-phase stretching vibrations. In the region 750–780 cm^{-1} a characteristic peak due to S-O stretching also appeared [157] (Figure 19 a). In the Raman spectrum, also a prominent peak at around 1100 cm^{-1} due to the SO_2 out-of-phase stretching was observed (Figure 19b). Thus, the FTIR and Raman data support the incorporation of sulfonated cellulose in the designed hydrogel beads.

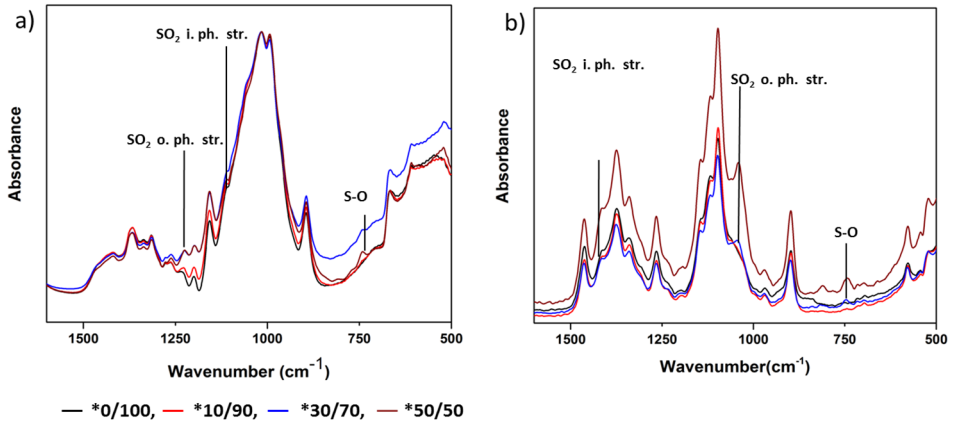

Figure 19. (**a**) Attenuated total reflectance-Fourier transform infrared (ATR-FTIR) and (**b**) Raman spectra of sulfonated cellulose hydrogel beads.

The ultrastructure and morphology of beads were studied by SEM technique. In case of bead prepared from Enoalfa HCS cellulose solution, the internal structure shows clear zonal demarcation in the cross-section of the bead (Figure 20). The surface skin is the outermost layer followed by loosely oriented network and a compact central zone. The formation of zones could be due to the continuous coagulation and ion exchange during phase separation process [158].

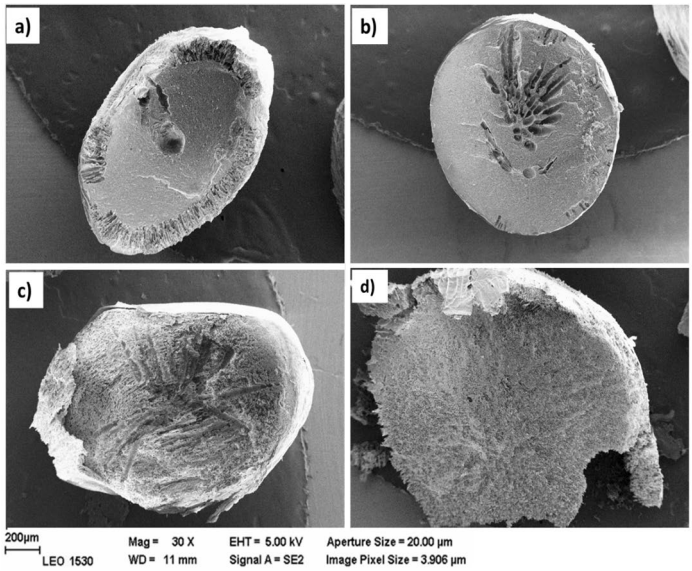

Figure 20. (a–d) Cross-section images of lyophilized *0/100, *10/90, *30/70, and *50/50 CES/Enoalfa-HyCellSolv hydrogel beads, respectively.

During the initial coagulation process, the rate of ion exchange is fast, resulting in outer skin and loose network formation. The compact central network structure could be due to the slow process of ion exchange after the system attained an equilibrium. In the case of CES blended beads, only two zones were observed. The outermost surface and the central compact zone. The reason for this could be the slower ion exchange rate between sodium ion attached to sulfonate groups and the acidic protons.

The higher magnification images of the hydrogel beads showed a trend of increasing surface smoothness and porosity with increasing concentration of CES polymer in the beads (Figure 21). For example, the *0/100 and*10/90 beads have compact network structure as compared to the *30/70 and *50/50 beads. This observation is directly related to the high concentration of Enoalfa HyCellSolv cellulose in the *0/100 and *10/90 blend solutions. It is presumed that, in 7 % NaOH-12 % urea aqueous solution, the HyCellSolv pulp is more coiled due to weak solvation and has stronger cohesive forces than the CES polymers in the same solvent system. Hence, Enoalfa HyCellSolv cellulose polymers approach towards

each other faster during coagulation in acid and the rapid coagulation process produces dense ultrastructures. While the coagulation of *30/70 and *50/50 blends with well-separated polymers due to the charge led to more porous ultrastructures. Thus, a high content of CES resulted in the higher water holding capacity due to the charged groups, which also controlled the porous structure in the beads.

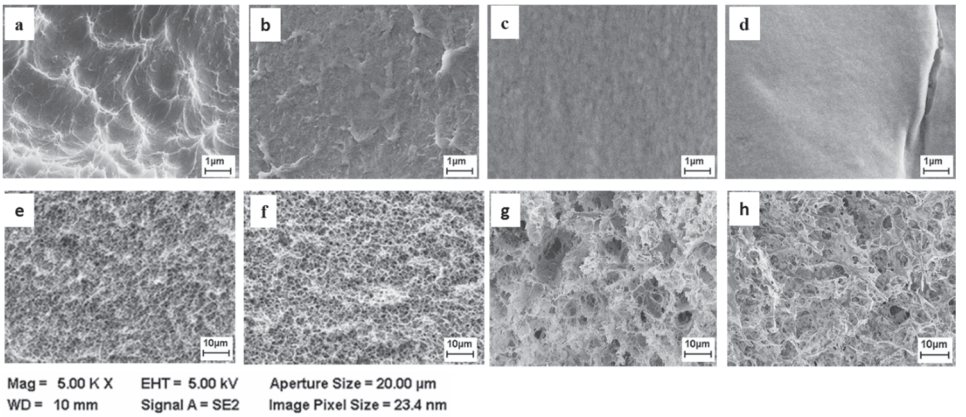

Figure 21. (a–d) surface morphology and (e–h) internal morphology of *0/100, *10/90, *30/70, and *50/50 CES/Enoalfa-HyCellSolv lyophilized hydrogel beads, respectively.

5.4 Effect of incorporating chitosan in the cellulose hydrogel beads and evaluation of cytocompatibility

5.4.1 Cellulose-chitosan blending and role of coagulating medium on the chemical composition of the hydrogel beads

Chitosan and cellulose were blended in NaOH/urea/water (7/12/81) solvent system with the following ratios 0/100, 10/90, 30/70, 50/50, 70/30, 90/10. Droplets of the blends were coagulated in the form of beads in 2M acetic acid (A), hydrochloric acid (B), and sulfuric acid (C) respectively. Thus, the hydrogel beads were named by the initial concentration of the chitosan added and the acid used. For example, the hydrogel with initial chitosan content 70% and coagulated in acetic acid was named as 70A. The chitosan-cellulose ratio up to 70/30 resulted in stable entities, which on further increasing chitosan content lead to unstable beads. In addition, the chosen coagulating medium played an important role in the final composition of the resulting hydrogel beads.

The elemental analysis results showed that amongst 70A, B and C type of beads, the 70A had the highest measured nitrogen content equivalent to 3.4 mmol/g. The 70B and 70C had 1.2 mmol/g and 2.9 mmol/g respectively

(Figure 22a). A relatively increasing trend in nitrogen content was also observed in all the beads coagulated in different acidic media with increasing chitosan content from 30 % to 70 %. The presence of chlorine and sulphur atoms was observed in the beads coagulated in hydrochloric and sulfuric acid (Figure 22 b –c).

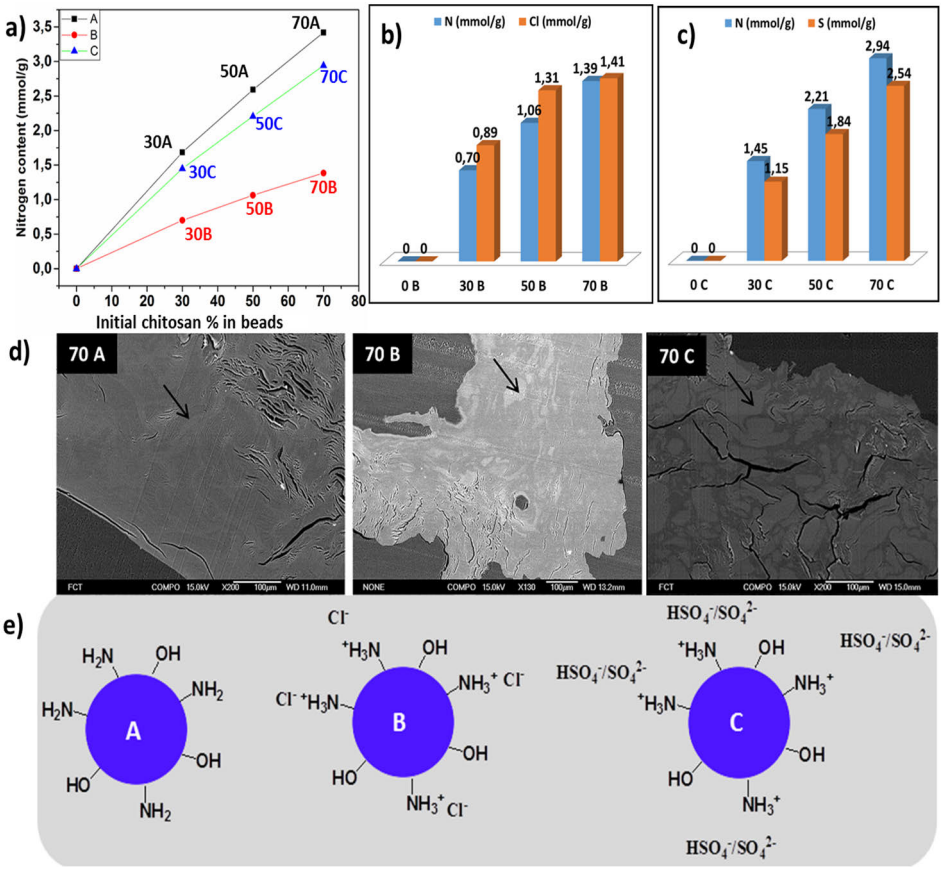

Figure 22. a) Total nitrogen content present in beads with varying chitosan composition coagulated in 2 M acetic acid (A), 2 M hydrochloric acid (B) and 2 M sulfuric acid (C). b-c) A comparison of chlorine and sulphur with the nitrogen content in B and C type. d) Nitrogen element distribution measured via spot analysis in 70A, 70B and 70C and **e)** Presentation of possible ionic interactions in A, B and C type.

It is percieved that the amino groups in the chitosan were ionically interacting with the chloride (Cl^-) and hydrogen sulfate (HSO_4^-) or sulfate (SO_4^{2-}) ions generated from the respective acids. The qualitative spot analysis of the beads via SEM-EDS showed that 70A beads had homogenous chitosan distribution while a non-homogenous pattern was observed in the 70B and 70C as shown in Figure (22 d). The proposed chemical constitution

of the hydrogel beads has been shown in (Figure 22 e). The pH of the coagulating medium had a key role in the retention and loss of chitosan from the hydrogel beads. In case of A-type beads, the measured pH of the coagulating medium was approximately 5. Thus resulting in reduced solubility of the chitosan and irreversible interaction with the cellulose polymer [159]. The lowest chitosan content was observed in B-type of hydrogel beads. It could be presumed that the final coagulating medium of the B-type, had a pH value of 1 and even low concentrations of HCl is enough to solubilize chitosan due to its strong acidic nature. In case of C type beads, it is clear that sulfuric acid does not lead to the dissolution of chitosan even after the protonation of amino groups (NH_3^+). It has been shown in a study, that in the presence of sulfuric acid, the amino groups of chitosan are protonated (NH_3^+) but are in strong electrostatic interaction with the sulfonate (SO_4^{2-}) anions [160]. Therefore, the coagulating medium plays a decisive role in retaining the chitosan in cellulose-chitosan hydrogel beads.

5.4.2 Analysis of chitosan retention and chemical changes in the hydrogel beads by ATR-FTIR, RAMAN and NMR spectroscopy

The ATR-FTIR analysis of the chitosan-cellulose hydrogel beads coagulated in 2 M acetic, hydrochloric and sulfuric acid displayed significant variations from the pristine chitosan and cellulose polymers. In chitosan- cellulose beads, the 3600-3000 cm^{-1} region which corresponds to OH stretching and NH vibrations, is broader in 70C than the 70A and **7**0B. Similarly, variations were observed in the amide and amino group vibrations region of 1700-1500 cm^{-1}. In 70A, 70B and 70C, the peak due to amide I (at 1641 cm^{-1}) overlaps with the water absorbance peak. The free amino groups band also displayed clear variations. In 70A, the band appeared at 1555 cm^{-1}, which is similar to the untreated chitosan. While in 70B, a band with lower intensity was observed with a slight shift towards the right at 1525 cm^{-1}. In the case of 70C beads, a peak at 1532 cm^{-1} of equal intensity and a small shift towards the right was observed. In the case of 70B and 70C, the shift in peaks towards the right is presumably related to the protonated amino (NH_3^+) groups bending vibrations which are involved in ionic interaction with the counterions [157]. At 1425 and 1374 cm^{-1} a slight variation in peaks due to CH deformations was also observed (Figure 23 a).

In the Raman spectra also, similar results were obtained. In 70A, the 3600-3100 cm^{-1} region displayed sharp peaks matching with that of chitosan, whereas 70B and 70C showed broader bands In 70A, the amide and the amino region matches with the pristine chitosan showing the presence of unmodified chitosan. In 70B, a comparatively less intensity band and in 70C a broadband was observed. The presumed reason of band broadening in 70C could be due to strong ionic interactions between the protonated amino groups and hydrogen sulfate or sulfonate anion.

In 70 C, a very characteristic peak due to the presence of sulfate (SO_4^{2-}) ions at 974 cm^{-1} was also apparent[157]. The role of sulfuric acid has also been explained by the fact that first, the sulfuric acid protonates the amino group and further acts as a crosslinking agent between the protonated amino groups by SO_4^{2-} ions[157]. Hence, the ATR-FTIR and Raman spectroscopic data confirmed the protonation of amino groups and interaction between the amino groups and negatively charged species in case of 70B and 70C hydrogel beads. While in 70A beads, no such evidence was observed.

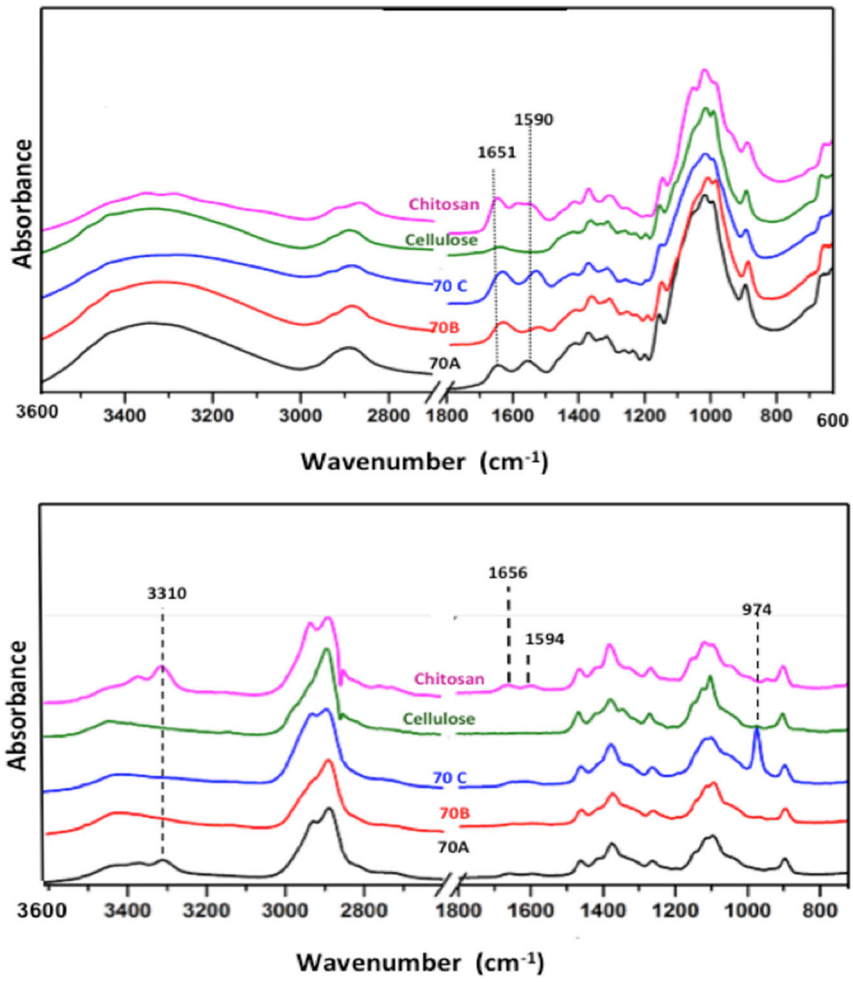

Figure 23. a) ATR- FTIR and b) Raman spectra of chitosan cellulose and 70**A**, 70**B** and 70**C** lyophilized hydrogel beads

The solid-state CP-MAS ^{13}C- and ^{15}N NMR NMR measurements of chitosan, cellulose, sulfuric acid treated chitosan reference samples, as well as the lyophilized hydrogel beads 70A, 70B and 70C were performed. In the CP-MAS ^{13}C NMR spectra of cellulose and chitosan (Figure 24 a) the

characteristic signals were observed which have been reported in the literature[161,162]. The major difference between cellulose and chitosan in the CP-MAS ^{13}C NMR spectra is the C-2 signal that is shifted to the (56 ppm) towards the higher field in chitosan as compared to cellulose (73 ppm). Also, the signals at 22 ppm (CH_3) and 173 ppm (C=O), corresponding to residual acetyl groups are observed in the CP-MAS ^{13}C NMR spectrum of chitosan. The sulfuric acid treated chitosan resulted in the protonation of the NH_2-groups, which are ionically interacting with sulfonate ions. This chemical crosslinking resulted in the broadening of all the signals observed in CP-MAS ^{13}C NMR spectra and shift of C1- and C4-signals (Figure 24 a). These observations are further supported by CP-MAS ^{15}N NMR spectra (Figure 24 b). The NH_2-signal in unmodified chitosan resonates at 22.6 ppm, whereas the nitrogen atoms in the NHOAc-groups resonates at 121.7 ppm.

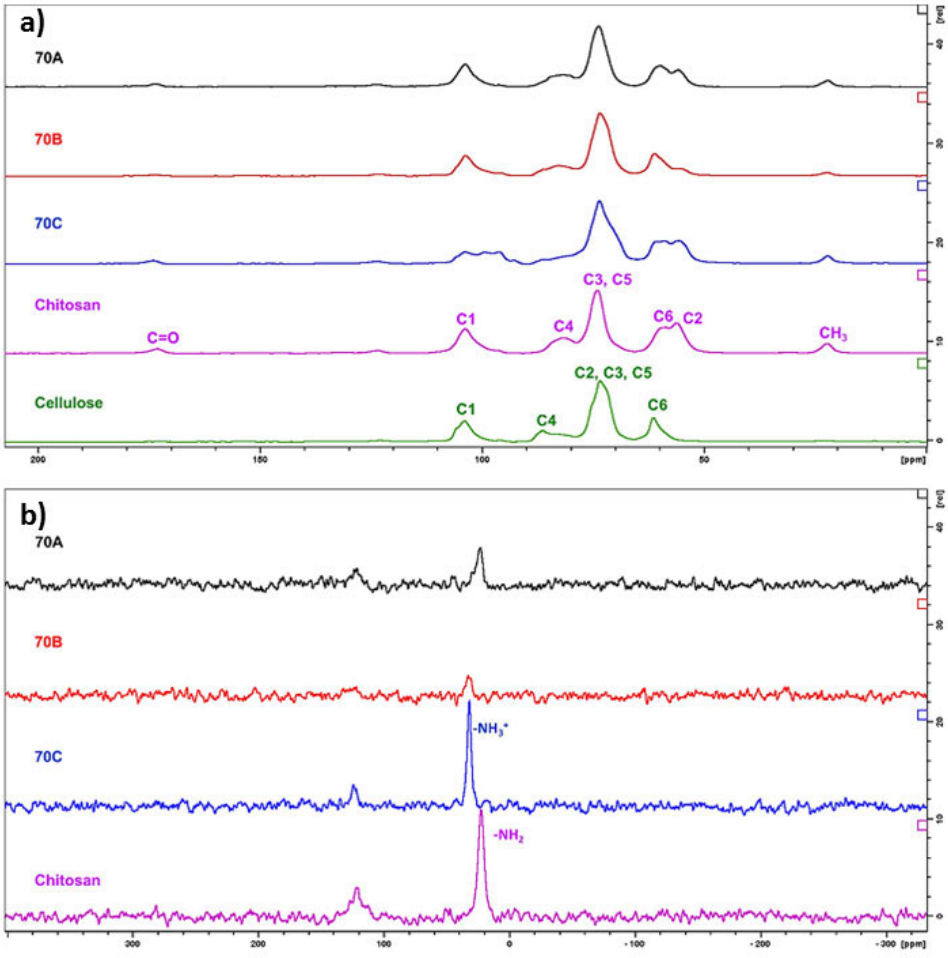

Figure 24. a) CP-MAS ^{13}C NMR spectra b) CP-MAS ^{15}N NMR spectra of chitosan, cellulose, 70A, 70B and 70C Chitosan-cellulose lyophilized hydrogel beads.

When chitosan is treated with sulfuric acid, the nitrogen atoms in the corresponding NH_3^+- groups resonates at 32.0 ppm, which is regarded as a clear indication of the modification of chitosan (Figure 25 b). The data of 70A shows that a physical mixture of cellulose and chitosan was present with no changes in the chemical structure. The 70B has low amount of chitosan and would be ambiguous to comment on any chemical changes in the chitosan, based upon the results.

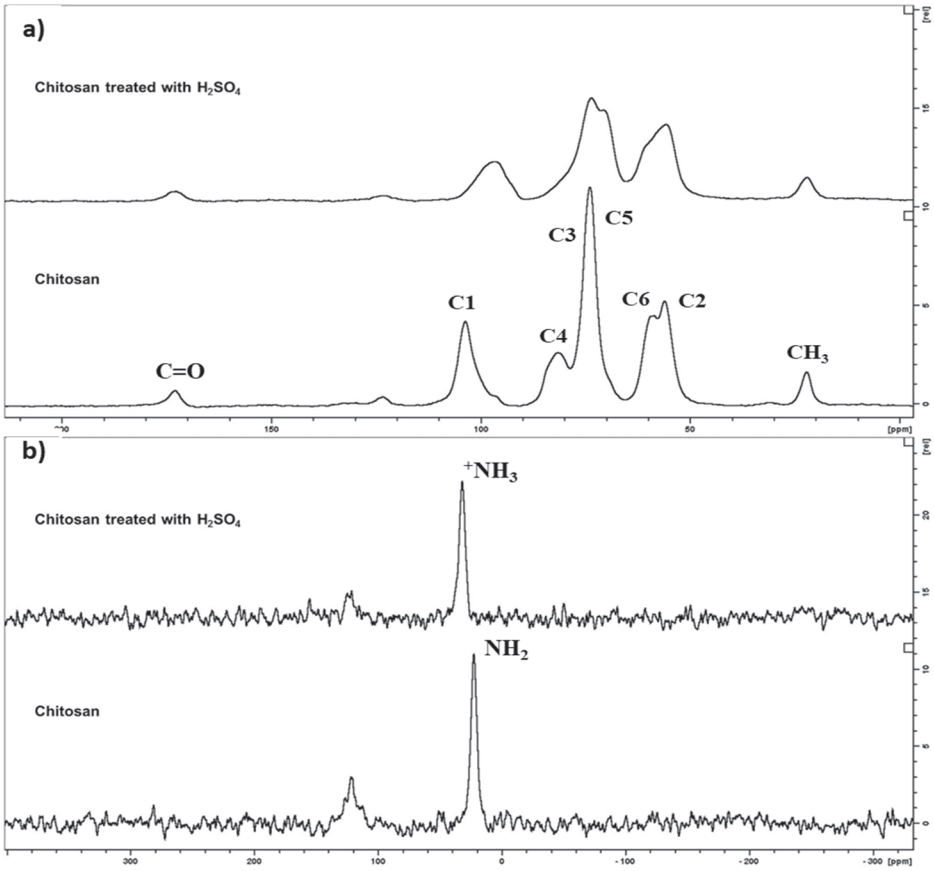

Figure 25 a). CP-MAS ^{13}C NMR spectra b) CP-MAS ^{15}N NMR spectra of chitosan and chitosan treated with sulfuric acid.

The main signal in the 70C and 70B, CP-MAS ^{15}N NMR spectra corresponds to the resonance frequency of NH_3^+- groups. This further strengthens the conclusion of ionic crosslinking of the chitosan in these hydrogel beads. The corresponding signal in the CP-MAS ^{15}N NMR spectra of 70A is at 22.6 ppm indicating that chitosan in this sample is not in ionic interaction with any counterion. Hence, the CP-MAS ^{13} C and ^{15} N NMR spectra support the results from IR and Raman spectroscopy.

5.4.3 Cytocompatibility evaluation of chitosan- cellulose hydrogel beads with MDA-MB-231 cells (Human breast adenocarcinoma-A soft Tissue organ)

The development of materials for soft tissue engineering applications requires special kind of cells, which have originated from a soft tissue organ. Therefore human breast adenocarcinoma cells (MDA-MB-231) which originate from the human female breast (a soft tissue organ), are potential model cells for evaluating the potential of the developed materials. In the study, WST-1 cell proliferation assay and MDA-MB-231 cells (human breast adenocarcinoma) were utilized to evaluate the initial cytocompatibility of 70A, 70B and 70C hydrogel beads over a period of 48h.

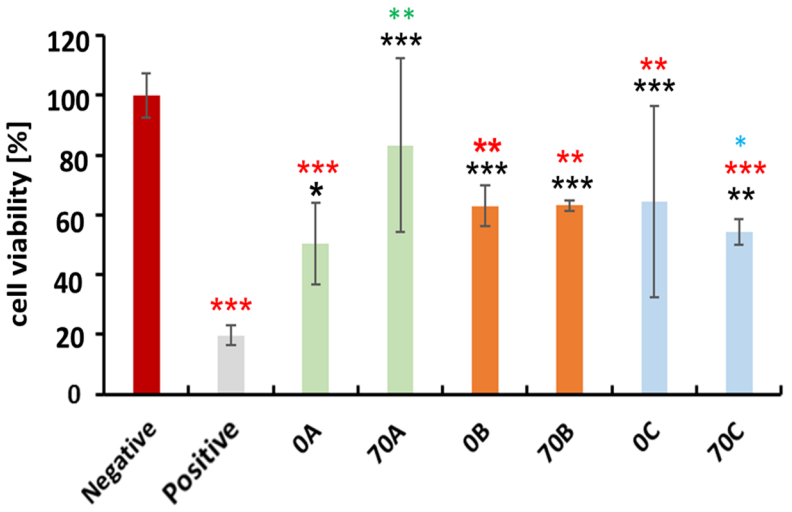

Figure 26. Human breast adenocarcinoma (MDA-MB-231) cytocompatibility result with 0A, 70A, 0B, 70B and 0C, 70C chitosan–cellulose hydrogel beads over the timeframe of 48h. Values are expressed as percentage of the means ± SD (n=4). Statistical significance was defined as *P<0.05 **P<0.01, ***P<0.005 compared to control samples (ANOVA test). Black * and red * indicates sample comparison to negative and positive control respectively. While green * shows comparison between 0A-70A, 0B-70B, 0C-70C and blue * shows between 70A-70B, 70A-70C, 70B-70C.

All the chosen hydrogel beads have shown to be cytocompatible with the exposed cells (Figure 26). Our aim was to find out the most cytocompatible hydrogel beads amongst all tested samples. A comparison between positive control (DMSO was choosen as positive control to cellular toxicity as it is toxic to the cells at higher concentrations) and 0A, 70A, 0B, 70B, 0C, 70C showed that all the hydrogel beads are non-toxic and cytocompatible. While in comparison to negative control the Advanced DMEM, all groups showed varied cytocompatibility. The comparison of 0A-70A shows that 70A type is

more cytocompatible than the 0A type. While no significant difference was observed between 0B-70B and 0C-70C. Further, a comparison between 70A-70B, no significant difference was observed. While in case of 70A-70C, the 70A type shown to be more cytocompatible than the 70C type. The presumed reason for these observations could be due to the presence of higher content of chitosan in the 70A hydrogel beads and absence of any counterions to interact with the amino groups. Thus making them suitable to interact with the cells[163]. While in the case of 70B and 70C, the amino groups are involved in ionic crosslinking with the chloride and sulfonate or hydrogen sulfate groups respectively. Therefore, resulting in the unavailability of the amino groups to interact with the cells. Hence, we can propose that amongst all tested hydrogel beads with the model cells for soft tissue engineering, the 70A type was comparatively more cytocompatible than the other hydrogel bead types.

5.4.4 Cytocompatibility evaluation of Chitosan-cellulose beads coagulated in acetic acid with human bone derived osteoblast cells (Hard Tissue)

In the field of bone, tissue engineering also, the biocompatibility is the prerequisite for any scaffold. Our objective in this study was also to evaluate the biocompatibility of the chitosan- cellulose hydrogel beads that were coagulated in acetic acid with human bone-derived osteoblast cells.

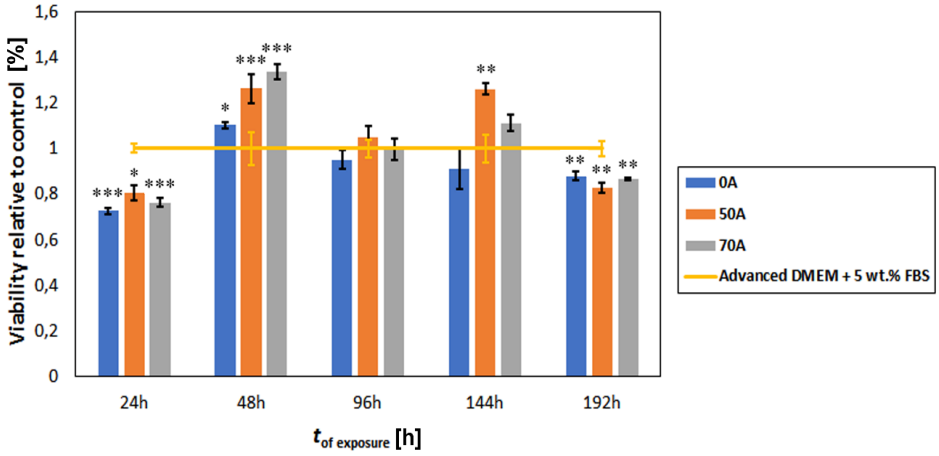

Figure 27. Osteoblast biocompatibility (proliferation behaviour) with 0A, 50A and 70A chitosan–cellulose hydrogel beads based on the MTT assay over the timeframe of 192h. The values are expressed as percentage of the means ± SD (n=4). Statistical significance was defined as *P<0.05, **P<0.005, ***P<0.001 compared to control sample (ANOVA test).

The comparative biocompatibility study results between the control sample, i.e., advanced DMEM, 0A, 50A and 70A at various times of exposure (up to 192h) are summarized in (Figure 27). The growth of the used cells has been affected by the hydrogel beads with varying time intervals. A lower viability of the cells grown together with the bead groups was observed at a period of 24h. Whereas after 48h, all prepared groups showed an increased viability, when compared to the control. Further after 96h and 144h, the viability was comparable to the control sample, showing that the beads were suitable for the growth of osteoblast cells at least up to 144h. After 192h a decrease in the viability of the cells exposed to the bead groups was observed when compared to the control groups was observed. The decrease in the viability of presumably not related to the toxic effect of beads, but could be due to the cells overgrowth in the P96 plate wells. Such an effect was not observed in the control samples. Therefore, it can proposed that the chitosan modified hydrogel bead outperform the pure cellulose beads, making them suitable for future testing in the development of materials for bone tissue engineering.

Conclusion

The objective of the supramolecular design of cellulose based hydrogel beads and the challenges involved have provided an understanding related to the mechanism occurring at the supramolecular level during the design of the hydrogel beads. The Dissolving pulp was selected as raw material to design the hydrogel beads in water based solvent systems. Therefore, the initial study provided a substantial information on the controlled depolymerisation of dissolving and kraft pulps utilizing acids with varying acidic strengths (pKa -10 to 4.7) in aqueous, ethanolic and a mixture of both solvent systems. Stronger acids resulted in lower DPυ values as compared to weaker acids. The addition of ethanol in the treatment liquor beyond 36 % concentration preserved the cellulose content. A remarkable effect of acid strength was also visible during the dissolution of treated fibres in 0.2 M CED. The stronger acid treated fibres dissolved via fragmentation while weaker acid treated fibres showed ballooning mechanism.

During the hydrogel beads design, pristine cellulose beads proved to be a potential candidate for futher chemical modification. The TEMPO mediated oxidation of the beads was a successful approach to introduce anionic charge and carbonyl moieties. The carbonyl group present was further explored to introduce cationic moiety by performing hydrazide coupling with carboxymethyl trimethylammonium chloride hydrazide reagent. The zwitterionc cellulose beads showed an increased water holding capacity and porosity as compared to the pristine and oxidized beads.

The sulfonated cellulose hydrogel beads designed provided an in depth understanding of the mechanism-playing role during the blending of a water-soluble ionic cellulose derivative (CES) with pretreated cellulose in sodiumhydroxide-urea-water solvent system and regeneration in 2M sulfuric acid. An increased concentration of CES from 10 % to 70 % in the blends displayed the trend of reducing viscosity and storage moduli (G´). The hydrogel beads upto 50 % initial CES concentration blended displayed physically stability with increased porosity and water holding capacity in comparision to pristine cellulose hydrogel beads.

The ease of the polymer blending approach was further explored to design of ionic chitosan cellulose based hydrogel beads. The blends of varying concentration of chitosan from 10 % to 90 % with the pretreated cellulose in sodiumhydroxide-urea-water solvent system were regenerated in 2M acetic, hydrochloric and sulfuric acid systems. The final chitosan content retention in the hydrogel beads as compared to the initial belnds was predominantly governed by the regenerating medium. The hydrogel beads regenerated in 2M acetic acid showed the retention of unmodified chitosan, while in 2M hydrochloric acid and 2M sulfuric acid ionic crosslinking was apparent between the protonated amino group and the respective anions. Also, the hydrogel beads with varying chitosan content

coagulated in 2M acetic acid showed highest chitosan content retention in the beads as compared to hydrochloric and sulphuric acid systems. The 70 % chitosan – 30 % cellulose hydrogel beads coagulated in 2M acetic acid also showed highest biocompatibility towards human breastadeno-carcinoma cells than the beads with same initial chitosan content coagulated in 2M hydrochloric and 2M sulphuric acid. These hydrogel beads have also shown promising biocompatibility with the human bone derived osteoblast cells.

Therefore, it can be concluded that, it is possible to design functional cellulose based biomaterials in the form of hydrogel beads either by polymer blending approach or by heterogenous chemical modification of the pristine cellulose beads. The solvent system employed for dissolution and blending of polymers, the chemical nature of the polymer blended with the cellulose, the molar ratio of the reagents used for heterogenous functionalization and the regenerating medium directly influences the properties of the hydrogel beads.

Future Prespective

Eventhough a lot of research has been done in the past to design natural polymer based hydrogels. Still there are small niches available for the researchers to explore in the future and address the unanswered questions. Therefore, cellulose and chitosan will always be the polysaccharides of priority due to abundant availability and exquisite properties such as non-toxicity, biodegradability and biocompatibility. The opportunity to tune the polymer properties such as polymer chain length from milli to micro to nanoscale, chemical functionalization at the molecular level to the supramolecular level, opens up a wide area for the research on the developemt and design of cellulose and chitosan based hydrogels. The solvent of choice, shaping methodolgy, regeneration mode, and post processing conditions, governs the processeability of these natural polymers into hydrogels. According to my opinion, designing of cellulose-based hydrogels by blending of polymers such as sodium cellulose ethylsulfonate and chitosan, as done in my research work, can significantly improve the hydrogels properties. Even the heterogeneous mode of function-nalization resulting in the generation of carboxylic and quaternary ammonium groups can also improve the hydrophilicity of the hydrogels. Therefore, the work compiled in the thesis will provide a base to work further in the area of supramolecular design of polysaccharide-based hydrogels and to futher evaluate the potential applications in tissue engineering area.

Acknowledgements

First, I would like to thank my supervisor Prof.Pedro Fardim for providing the opportunity to work in his research group. The independent research atmosphere helped me to grow as a researcher. The PShpaes project was a platform to learn and perform research activities along with project coordination and collaboration with the international partners.

I am thankful to Prof. Zhiming Liu for reviewing my thesis and Prof. Monika Ek for being my reviewer and also my opponent

I am deeply thankful to Dr. Jan Gustafsson for being my co-supervisor. Things would not have been so fast and easy without your help.

A big thank to Dr. Jani Trygg for his support and guidance during the research work. It was a great association to cherish for lifetime. I would like to acknowledge all my FCT colleagues, Konstantin Gabov for being a nice friend from the very first day we started sharing the same sitting place, Olga Gabov for sharing your experience of thesis writing to final dissertation planning and management. Thanks to Liji Shobhandas for sharing good time and conversations and also supporting during UNO sessions. Thanks to Jasmina Obradovic, Beatriz Vega, and Carl Lange for being great and helpful colleagues. Thanks to Thomas Holmblom and Annika also. I enjoyed coffee sessions and discussions with you guys. I would like to thank Agneta Hermansson and Marika Ginnman for all the support from stationary to the successful travel plans and reimbursements. I am also thankful to Björn Friberg (Avya), Peter Holmund and Paulina Saloranta for their support.

I am deeply thankful to Docent Dr. Tiina Saloranta -Simell for her efforts with NMR and all critical evaluation of the work we did together.

I would like to thank the PShapes project colleagues Prof. Thomas Heinze, Martin Gericke, Jens Schaller, Tamil Selvan Mohan, and Silvo Hribernik for being great people to work and share the knowledge. I have learnt a lot from you all.

The staff of 3PK and PAF is acknowledged for their support and interactive sessions especially during Christmas and glogs party. I am thankful to Jarl Hemming for all the help during GCMS experiments and data analysis.

I also want to thank the Prof. Esa-Matti Lilius and Janne Atosuo from Immunochemistry group- UTU to allow me to work in their laboratory.

I am also thankful to the TEKES and Wood Wisdom for financial support during the research.

Thanks to all my friends who are in Turku and who have moved away. Preety & Santosh, Amruta & Prasanna, Aman & Hasan, Rohini-Mahesh, Sangeeta-Himanshu, Swathi & Kalyan, Raghu-Yashu, Nitin & Avlokita, Ankitha, Vipin, Rajesh, Madhukar, Vinay & Deepika. Weekends and special moments would have not been so enjoyable without you people. In addition, my girlies Uzma, Sana and Priyanka thanks for being there and sharing

experiences on all the aspects from cooking to selecting the right wear for the kid.

I am thankful to my parents for always supporting, encouraging and believing in me. Whatever I am, it is all because of you. You are my strength and role model as a parent for my child. Thanks to my sisters Jiya and Bittu for always being by my side and love to my daksh and pihoo. I am also grateful to my in Laws for their love and support.

At last, thanks to my better half (Subhash Tripathi). You are the charm of my life. It has been a great journey with you, many more to come and love has now another name that is our son Devvrat. I love to listen, the way you address us...Mama and baba. You are our lifeline.

Poonam Trivedi
Åbo, March 2019

Bibliography

1. Budtova, T. & Navard, P. Cellulose in NaOH–water based solvents: a review. *Cellulose* **23,** 5–55 (2016).
2. Taherzadeh, M. J. & Karimi, K. ACID-BASED HYDROLYSIS PROCESSES FOR ETHANOL FROM LIGNOCELLULOSIC MATERIALS: A REVIEW. *BioResources* **2,** 472–499 (2007).
3. Lennartsson, P. R., Niklasson, C. & Taherzadeh, M. J. A pilot study on lignocelluloses to ethanol and fish feed using NMMO pretreatment and cultivation with zygomycetes in an air-lift reactor. *Bioresour. Technol.* **102,** 4425–32 (2011).
4. Thakur, V. K., Thakur, M. K. & Gupta, R. K. Graft Copolymers from Natural Polymers Using Free Radical Polymerization. *Int. J. Polym. Anal. Charact.* **18,** 495–503 (2013).
5. Heinze, T. & Liebert, T. Unconventional methods in cellulose functionalization. *Prog. Polym. Sci.* **26,** 1689–1762 (2001).
6. Payen, A. Mémoire sur la composition du tissu propre des plantes et du ligneux. (Memoir on the composition of the tissue of plants and of woody [material]). Comptes Rendus Hebdomadaires des Séances de l'Académie des Sci-ences, 7, 7. - References - Scientific Resear. *Compt. Rend. Acad. Sci.* **7,** 1052 (1838).
7. Robinson, C. Die hochpolymeren organischen verbindungen-kautschuk und cellulose: H. Staudinger Springer-Verlag: New Impression, Berlin, 1960. (xvi+540 pp.; 612in. by 10 in.), DM 59.00. *Polymer (Guildf).* **3,** 243–245 (1962).
8. Heinze, T., Liebert, T. & Koschella, A. *Esterification of polysaccharides*. (Springer, 2006).
9. Kroon-Batenburg, L. M. & Kroon, J. The crystal and molecular structures of cellulose I and II. *Glycoconj. J.* **14,** 677–90 (1997).
10. Šauperl, O., Stana-Kleinschek, K. & Ribitsch, V. Cotton Cellulose 1, 2, 3, 4 Buthanetetracarboxylic Acid (BTCA) Crosslinking Monitored by some Physical—chemical Methods. *Text. Res. J.* **79,** 780–791 (2009).
11. Revol, J.-F. & Goring, D. A. I. On the mechanism of the mercerization of cellulose in wood. *J. Appl. Polym. Sci.* **26,** 1275–1282 (1981).
12. Yoshiharu Nishiyama, †, Paul Langan, *,‡ and & Chanzy§, H. Crystal Structure and Hydrogen-Bonding System in Cellulose Iβ from Synchrotron X-ray and Neutron Fiber Diffraction. (2002).
13. Ciacco, G. T., Morgado, D. L., Frollini, E., Possidonio, S. & El Seoud, O. A. Some aspects of acetylation of untreated and mercerized sisal cellulose. *J. Braz. Chem. Soc.* **21,** 71–77 (2010).
14. Dinand, E., Vignon, M., Chanzy, H. & Heux, L. Mercerization of primary wall cellulose and its implication for the conversion of cellulose I→cellulose II. *Cellulose* **9,** 7–18 (2002).

15. Liu, Y. & Hu, H. X-ray diffraction study of bamboo fibers treated with NaOH. *Fibers Polym.* **9,** 735–739 (2008).

16. Wada, M., Chanzy, H., Nishiyama, Y. & Langan, P. Cellulose III ı Crystal Structure and Hydrogen Bonding by Synchrotron X-ray and Neutron Fiber Diffraction. *Macromolecules* **37,** 8548–8555 (2004).

17. M. Wada, † *et al.* Improved Structural Data of Cellulose IIII Prepared in Supercritical Ammonia. (2001).

18. Hutino, K. & Sakurada, I. Uber die Existenz einer vierten Modifikation der Cellulose. *Naturwissenschaften* **28,** 577–578 (1940).

19. Masahisa Wada, †,*, Laurent Heux, ‡ and & Sugiyama§, J. Polymorphism of Cellulose I Family: Reinvestigation of Cellulose IVI. (2004).

20. O'SULLIVAN, A. C. Cellulose: the structure slowly unravels. *Cellulose* **4,** 173–207 (1997).

21. O'Dell, W. B., Baker, D. C. & McLain, S. E. Structural Evidence for Inter-Residue Hydrogen Bonding Observed for Cellobiose in Aqueous Solution. *PLoS One* **7,** e45311 (2012).

22. Kennedy, J. F. & Pons, R. J. S. Cellulose: Structure, accessibility and reactivity: Hans A. Krassig, Gordon and Breach Science Publishers, South Africa, 1993. xvi + 376 pp. Price £169.00. ISBN 2-88124-798-9. *Carbohydr. Polym.* **26,** 313–314 (1995).

23. Klemm, D. *et al. Comprehensive cellulose chemistry. Vol. 1, Fundamentals and analytical methods*. (Wiley-VCH, 1998).

24. Wertz, J.-L., Bédué, O. & Mercier, J.-P. *Cellulose science and technology*. (EPFL Press, 2010).

25. *Handbook of Pulp*. (Wiley-VCH Verlag GmbH, 2006).

26. Himmel, M. E. *et al.* Biomass Recalcitrance: Engineering Plants and Enzymes for Biofuels Production. *Science (80-.).* **315,** 804–807 (2007).

27. Chandra, R. P. *et al.* Substrate Pretreatment: The Key to Effective Enzymatic Hydrolysis of Lignocellulosics? in *Biofuels* **108,** 67–93 (Springer Berlin Heidelberg, 2007).

28. Zhang, Y.-H. P. & Lynd, L. R. Toward an aggregated understanding of enzymatic hydrolysis of cellulose: Noncomplexed cellulase systems. *Biotechnol. Bioeng.* **88,** 797–824 (2004).

29. Harmsen, P. F. H., Huijgen, W. J. J., Bermúdez López, L. M. & Bakker, R. R. C. Literature Review of Physical and Chemical Pretreatment Processes for Lignocellulosic Biomass. (2010).

30. Mosier, N. S. *et al.* Industrial Scale-Up of pH-Controlled Liquid Hot Water Pretreatment of Corn Fiber for Fuel Ethanol Production. *Appl. Biochem. Biotechnol.* **125,** 077–098 (2005).

31. Mok, W. S. L. & Antal, M. J. Uncatalyzed solvolysis of whole biomass hemicellulose by hot compressed liquid water. *Ind. Eng. Chem. Res.* **31,** 1157–1161 (1992).

32. Chen, Y., Sharma-Shivappa, R. R., Keshwani, D. & Chen, C. Potential of Agricultural Residues and Hay for Bioethanol Production. *Appl. Biochem. Biotechnol.* **142,** 276–290 (2007).

33. Kootstra, A. M. J., Beeftink, H. H., Scott, E. L. & Sanders, J. P. Optimization of the dilute maleic acid pretreatment of wheat straw. *Biotechnol. Biofuels* **2,** 31 (2009).

34. Sun, Y. & Cheng, J. Hydrolysis of lignocellulosic materials for ethanol production: a review. *Bioresour. Technol.* **83,** 1–11 (2002).

35. González Villarreal, L. M. & Universidad de Guadalajara. Instituto de Botánica. *Contribución al conocimiento del género Quercus (Fagaceae) en el Estado de Jalisco*. (Instituto de Botánica, Universidad de Guadalajara, 1986).

36. Kim, S. & Holtzapple, M. T. Lime pretreatment and enzymatic hydrolysis of corn stover. *Bioresour. Technol.* **96,** 1994–2006 (2005).

37. Kim, T. H. & Lee, Y. Y. Pretreatment of corn stover by soaking in aqueous ammonia. *Appl. Biochem. Biotechnol.* **121–124,** 1119–31 (2005).

38. Ghose, T. K., Pannir Selvam, P. V. & Ghosh, P. Catalytic solvent delignification of agricultural residues: Organic catalysts. *Biotechnol. Bioeng.* **25,** 2577–2590 (1983).

39. Schmidt, A. S. & Thomsen, A. B. Optimization of wet oxidation pretreatment of wheat straw. *Bioresour. Technol.* **64,** 139–151 (1998).

40. Payal, R. S., Bejagam, K. K., Mondal, A. & Balasubramanian, S. Dissolution of Cellulose in Room Temperature Ionic Liquids: Anion Dependence. *J. Phys. Chem. B* **119,** 1654–1659 (2015).

41. Mora-Pale, M., Meli, L., Doherty, T. V., Linhardt, R. J. & Dordick, J. S. Room temperature ionic liquids as emerging solvents for the pretreatment of lignocellulosic biomass. *Biotechnol. Bioeng.* **108,** 1229–1245 (2011).

42. Häkansson, H. & Ahlgren, P. Acid hydrolysis of some industrial pulps: effect of hydrolysis conditions and raw material. *Cellulose* **12,** 177–183 (2005).

43. Sescousse, R. & Budtova, T. Influence of processing parameters on regeneration kinetics and morphology of porous cellulose from cellulose–NaOH–water solutions. *Cellulose* **16,** 417–426 (2009).

44. Trygg, J., Fardim, P., Gericke, M., Mäkilä, E. & Salonen, J. Physicochemical design of the morphology and ultrastructure of cellulose beads. *Carbohydr. Polym.* **93,** 291–299 (2013).

45. Cuissinat, C. & Navard, P. Swelling and Dissolution of Cellulose Part 1: Free Floating Cotton and Wood Fibres in N-Methylmorpholine-N-oxide–Water Mixtures. *Macromol. Symp.* **244,** 1–18 (2006).

46. *Cellulose Solvents: For Analysis, Shaping and Chemical Modification*. **1033,** (American Chemical Society, 2010).

47. Gericke, M., Fardim, P. & Heinze, T. Ionic Liquids — Promising but Challenging Solvents for Homogeneous Derivatization of Cellulose. *Molecules* **17,** 7458–7502 (2012).

48. Sixta. Ioncell-F: A High-strength regenerated cellulose fibre. *Nord. Pulp Pap. Res. J.* **30,** 043–057 (2015).

49. Ma, Y. *et al.* High-Strength Composite Fibers from Cellulose-Lignin Blends Regenerated from Ionic Liquid Solution. *ChemSusChem* **8,** 4030–4039 (2015).

50. Cuissinat, C. & Navard, P. Swelling and Dissolution of Cellulose Part II: Free Floating Cotton and Wood Fibres in NaOH–Water–Additives Systems. *Macromol. Symp.* **244,** 19–30 (2006).

51. Cuissinat, C., Navard, P. & Heinze, T. Swelling and dissolution of cellulose. Part IV: Free floating cotton and wood fibres in ionic liquids. *Carbohydr. Polym.* **72,** 590–596 (2008).

52. Cai, J. & Zhang, L. Rapid Dissolution of Cellulose in LiOH/Urea and NaOH/Urea Aqueous Solutions. *Macromol. Biosci.* **5,** 539–548 (2005).

53. Qi, H., Liebert, T. & Heinze, T. Homogenous synthesis of 3-allyloxy-2-hydroxypropyl-cellulose in NaOH/urea aqueous system. *Cellulose* **19,** 925–932 (2012).

54. Egal, M., Budtova, T. & Navard, P. Structure of aqueous solutions of microcrystalline cellulose/sodium hydroxide below 0 °C and the limit of cellulose dissolution. *Biomacromolecules* **8,** 2282–2287 (2007).

55. Cai, J. *et al.* Dynamic self-assembly induced rapid dissolution of cellulose at low temperatures. *Macromolecules* **41,** 9345–9351 (2008).

56. Qi, H., Chang, C. & Zhang, L. Effects of temperature and molecular weight on dissolution of cellulose in NaOH/urea aqueous solution. *Cellulose* **15,** 779–787 (2008).

57. El Seoud, O. A. & Heinze, T. Organic Esters of Cellulose: New Perspectives for Old Polymers. in 103–149 (2005).

58. Schmidt, S., Liebert, T. & Heinze, T. Synthesis of soluble cellulose tosylates in an eco-friendly medium. *Green Chem.* **16,** 1941–1946 (2014).

59. Zhou, D., Zhang, L., Zhou, J. & Guo, S. Cellulose/chitin beads for adsorption of heavy metals in aqueous solution. *Water Res.* **38,** 2643–2650 (2004).

60. Kim, J., Wang, N., Chen, Y., Lee, S.-K. & Yun, G.-Y. Electroactive-paper actuator made with cellulose/NaOH/urea and sodium alginate. *Cellulose* **14,** 217–223 (2007).

61. Gericke, M. *et al.* Studies on the tosylation of cellulose in mixtures of ionic liquids and a co-solvent. *Carbohydr. Polym.* **89,** 526–36 (2012).

62. Heinze, T., Rahn, K., Jaspers, M. & Berghmans, H. Thermal studies on homogeneously synthesized cellulosep-toluenesulfonates. *J. Appl. Polym. Sci.* **60,** 1891–1900 (1996).

63. Heinze, T. *Polysaccharides I : structure, characterisation and use*. (Springer, 2005).

64. Elschner, T. & Heinze, T. Cellulose Carbonates: A Platform for Promising Biopolymer Derivatives With Multifunctional Capabilities. *Macromol. Biosci.* **15,** 735–746 (2015).

65. Fraczyk, J., Kolesinska, B., Relich, I. & J., Z. Cellulose Functionalysed with Grafted Oligopeptides. in *Cellulose - Medical, Pharmaceutical and Electronic Applications* (InTech, 2013).

66. Lindh, J., Carlsson, D. O., Strømme, M. & Mihranyan, A. Convenient One-Pot Formation of 2,3-Dialdehyde Cellulose Beads via Periodate Oxidation of Cellulose in Water. *Biomacromolecules* **15,** 1928–1932 (2014).

67. Lindh, J., Ruan, C., Strømme, M. & Mihranyan, A. Preparation of Porous Cellulose Beads via Introduction of Diamine Spacers. *Langmuir* **32,** 5600–5607 (2016).

68. Gericke, M., Trygg, J. & Fardim, P. Functional Cellulose Beads: Preparation, Characterization, and Applications. *Chem. Rev.* **113,** 4812–4836 (2013).

69. Zhou, X. *et al.* Effect of the degree of substitution on the hydrophobicity of acetylated cellulose for production of liquid marbles. *Cellulose* **23,** 811–821 (2016).

70. Cellulose ethylsulfonate-based absorbent material. (2009).

71. Isogai, A., Saito, T. & Fukuzumi, H. TEMPO-oxidized cellulose nanofibers. *Nanoscale* **3,** 71–85 (2011).

72. Hirota, M., Tamura, N., Saito, T. & Isogai, A. Oxidation of regenerated cellulose with NaClO2 catalyzed by TEMPO and NaClO under acid-neutral conditions. *Carbohydr. Polym.* **78,** 330–335 (2009).

73. de Carvalho, R. A. *et al.* The potential of TEMPO-oxidized nanofibrillar cellulose beads for cell delivery applications. *Cellulose* **23,** 3399–3405 (2016).

74. Weishaupt, R. *et al.* TEMPO-Oxidized Nanofibrillated Cellulose as a High Density Carrier for Bioactive Molecules. *Biomacromolecules* **16,** 3640–3650 (2015).

75. Heinze, T., Genco, T., Petzold-Welcke, K. & Wondraczek, H. Synthesis and characterization of aminocellulose sulfates as novel ampholytic polymers. *Cellulose* **19,** 1305–1313 (2012).

76. Elschner, T. & Heinze, T. A promising cellulose-based polyzwitterion with pH-sensitive charges. *Beilstein J. Org. Chem.* **10,** 1549–1556 (2014).

77. Elschner, T. *et al.* Zwitterionic Cellulose Carbamate with Regioselective Substitution Pattern: A Coating Material Possessing Antimicrobial Activity. *Macromol. Biosci.* **16,** 522–534 (2016).

78. Madihally, S. V & Matthew, H. W. Porous chitosan scaffolds for tissue engineering. *Biomaterials* **20,** 1133–42 (1999).

79. Rane, K. D. & Hoover, D. G. Production of Chitosan by fungi. *Food Biotechnol.* **7,** 11–33 (1993).

80. Aranaz, I., Harris, R. & Heras, A. Chitosan Amphiphilic Derivatives. Chemistry and Applications. *Curr. Org. Chem.* **14,** 308–330 (2010).

81. Aranaz, I. *et al.* Functional Characterization of Chitin and Chitosan. *Curr. Chem. Biol.* **3,** 203–230 (2009).

82. Leedy, M. R. *et al.* Use of Chitosan as a Bioactive Implant Coating for Bone-Implant Applications. in 129–165 (Springer, Berlin, Heidelberg, 2011).

83. Jayakumar, R. (Rangasamy), Prabaharan, M., Muzzarelli, R. A. A. & Bumgardner, J. D. *Chitosan for biomaterials II*. (Springer, 2011).

84. Rinaudo, M. Chitin and chitosan: Properties and applications. *Prog. Polym. Sci.* **31,** 603–632 (2006).

85. Pavinatto, F. J., Caseli, L. & Oliveira, O. N. Chitosan in Nanostructured Thin Films. *Biomacromolecules* **11,** 1897–1908 (2010).

86. Takahashi, T., Takayama, K., Machida, Y. & Nagai, T. Characteristics of polyion complexes of chitosan with sodium alginate and sodium polyacrylate. *Int. J. Pharm.* **61,** 35–41 (1990).

87. Sudarshan, N. R., Hoover, D. G. & Knorr, D. Antibacterial action of chitosan. *Food Biotechnol.* **6,** 257–272 (1992).

88. Ong, S.-Y., Wu, J., Moochhala, S. M., Tan, M.-H. & Lu, J. Development of a chitosan-based wound dressing with improved hemostatic and antimicrobial properties. *Biomaterials* **29,** 4323–4332 (2008).

89. Lehr, C.-M., Bouwstra, J. A., Schacht, E. H. & Junginger, H. E. In vitro evaluation of mucoadhesive properties of chitosan and some other natural polymers. *Int. J. Pharm.* **78,** 43–48 (1992).

90. Yang, J. *et al.* Effect of chitosan molecular weight and deacetylation degree on hemostasis. *J. Biomed. Mater. Res. Part B Appl. Biomater.* **84B,** 131–137 (2008).

91. Dutta, P. K., Rinki, K. & Dutta, J. Chitosan: A Promising Biomaterial for Tissue Engineering Scaffolds. in 45–79 (Springer, Berlin, Heidelberg, 2011).

92. Dong, R., Pang, Y., Su, Y. & Zhu, X. Supramolecular hydrogels: synthesis, properties and their biomedical applications. *Biomater. Sci.* (2015).

93. Hamidi, M., Azadi, A. & Rafiei, P. Hydrogel nanoparticles in drug delivery. *Adv. Drug Deliv. Rev.* **60,** 1638–1649 (2008).

94. Sangeetha, N. M. & Maitra, U. Supramolecular gels: Functions and uses. *Chem. Soc. Rev.* **34,** 821 (2005).

95. Li, M. *et al.* Quasi-solid state dye-sensitized solar cells based on pyridine or imidazole containing copolymer chemically crosslinked gel electrolytes. *Chinese Sci. Bull.* **52,** 2320–2325 (2007).

96. Otsuka, E., Kudo, S., Sugiyama, M. & Suzuki, A. Effects of microcrystallites on swelling behavior in chemically crosslinked poly(vinyl alcohol) gels. *J. Polym. Sci. Part B Polym. Phys.* **49,** 96–102 (2011).

97. Jannasch, P. Physically crosslinked gel electrolytes based on a self-assembling ABA triblock copolymer. *Polymer (Guildf).* **43,** 6449–6453 (2002).

98. Sakasegawa, D., Goto, M. & Suzuki, A. Adhesion properties of physically crosslinked elastic gels of poly(sodium acrylate)–poly(acrylic acid) mixtures evaluated by a point contact method. *Colloid Polym. Sci.* **287,** 1281–1293 (2009).

99. Yang, Z. & Ding, J. A Thermosensitive and Biodegradable Physical Gel with Chemically Crosslinked Nanogels as the Building Block. *Macromol. Rapid Commun.* **29,** 751–756 (2008).

100. Chang, C. & Zhang, L. Cellulose-based hydrogels: Present status and application prospects. *Carbohydr. Polym.* **84,** 40–53 (2011).

101. Qiu, X. & Hu, S. "Smart" Materials Based on Cellulose: A Review of the Preparations, Properties, and Applications. *Materials (Basel).* **6,** 738–781 (2013).

102. Liu, C., Thormann, E., Claesson, P. M. & Tyrode, E. Surface Grafted Chitosan Gels. Part II. Gel Formation and Characterization. *Langmuir* **30,** 8878–8888 (2014).

103. Naumov, S., Knolle, W., Becher, J., Schnabelrauch, M. & Reichelt, S. Electron-beam generated porous dextran gels: Experimental and quantum chemical studies. *Int. J. Radiat. Biol.* **90,** 503–511 (2014).

104. Agulhon, P., Robitzer, M., Habas, J.-P. & Quignard, F. Influence of both cation and alginate nature on the rheological behavior of transition metal alginate gels. *Carbohydr. Polym.* **112,** 525–531 (2014).

105. Qiu, X. & Hu, S. "Smart" Materials Based on Cellulose: A Review of the Preparations, Properties, and Applications. *Materials (Basel).* **6,** 738–781 (2013).

106. Karaaslan, A. M., Tshabalala, M. A., and Buschle-Diller, G. Wood hemicellulose/chitosan-based semi-interpenetrating network hydrogels: Mechanical, swelling and controlled drug release properties. *Bioresources* **5,** 1036–1054 (2010).

107. Liang, X., Huang, Z., Zhang, Y., Hu, H. & Liu, Z. Synthesis and properties of novel superabsorbent hydrogels with mechanically activated sugarcane bagasse and acrylic acid. *Polym. Bull.* **70,** 1781–1794 (2013).

108. Kumari, M. & Chauhan, G. S. Adsorption capacity, kinetics, and mechanism of copper(II) uptake on gelatin-based hydrogels. *J. Appl. Polym. Sci.* **119,** 363–370 (2011).

109. Bajpai, A. K. & Mishra, A. Carboxymethyl cellulose (CMC) based semi-IPNs as carriers for controlled release of ciprofloxacine: an in-vitro dynamic study. *J. Mater. Sci. Mater. Med.* **19,** 2121–2130 (2008).

110. Li, N. & Bai, R. Copper adsorption on chitosan–cellulose hydrogel beads: behaviors and mechanisms. *Sep. Purif. Technol.* **42,** 237–247 (2005).

111. Way, A. E., Hsu, L., Shanmuganathan, K., Weder, C. & Rowan, S. J. pH-Responsive Cellulose Nanocrystal Gels and Nanocomposites. *ACS Macro Lett.* **1,** 1001–1006 (2012).

112. Ye, S. H., Watanabe, J., Iwasaki, Y. & Ishihara, K. Antifouling blood purification membrane composed of cellulose acetate and phospholipid polymer. *Biomaterials* **24,** 4143–52 (2003).

113. Sannino, A. *et al.* Biomedical application of a superabsorbent hydrogel for body water elimination in the treatment of edemas. *J. Biomed. Mater. Res.* **67A,** 1016–1024 (2003).

114. Cai, J and Zhang, L. Unique Gelation Behavior of Cellulose in NaOH/Urea Aqueous Solution. *Biomacromolecules* **7,** 183–189 (2006).

115. Turbak, A. F., Snyder, F. W. & Sandberg, K. R. Microfibrillated cellulose, a new cellulose product: properties, uses, and commercial potential. *J. Appl. Polym. Sci. Appl. Polym. Symp.; (United States)* **37,** (1983).

116. Domingues, R. M. A. *et al.* Development of Injectable Hyaluronic Acid/Cellulose Nanocrystals Bionanocomposite Hydrogels for Tissue Engineering Applications. *Bioconjug. Chem.* **26,** 1571–1581 (2015).

117. Köhnke, T., Elder, T., Theliander, H. & Ragauskas, A. J. Ice templated and cross-linked xylan/nanocrystalline cellulose hydrogels. *Carbohydr. Polym.* **100,** 24–30 (2014).

118. Dash, R., Foston, M. & Ragauskas, A. J. Improving the mechanical and thermal properties of gelatin hydrogels cross-linked by cellulose nanowhiskers. *Carbohydr. Polym.* **91,** 638–645 (2013).

119. Chau, M. *et al.* Composite Hydrogels with Tunable Anisotropic Morphologies and Mechanical Properties. *Chem. Mater.* **28,** 3406–3415 (2016).

120. Shen, X., Shamshina, J. L., Berton, P., Gurau, G. & Rogers, R. D. Hydrogels based on cellulose and chitin: fabrication, properties, and applications. *Green Chem.* **18,** 53–75 (2016).

121. Ninan, N. *et al.* Pectin/carboxymethyl cellulose/microfibrillated cellulose composite scaffolds for tissue engineering. *Carbohydr. Polym.* **98,** 877–885 (2013).

122. Yang, G., Zhang, L., Peng, T. & Zhong, W. Effects of Ca2+ bridge cross-linking on structure and pervaporation of cellulose/alginate blend membranes. *J. Memb. Sci.* **175,** 53–60 (2000).

123. Nishio, Y. & Manley, R. S. J. Cellulose-poly(vinyl alcohol) blends prepared from solutions in N,N-dimethylacetamide-lithium chloride. *Macromolecules* **21,** 1270–1277 (1988).

124. Liang, S., Wu, J., Tian, H., Zhang, L. & Xu, J. High-Strength Cellulose/Poly(ethylene glycol) Gels. *ChemSusChem* **1,** 558–563 (2008).

125. Chang, C., Peng, J., Zhang, L. & Pang, D.-W. Strongly fluorescent hydrogels with quantum dots embedded in cellulose matrices. *J. Mater. Chem.* **19,** 7771 (2009).

126. Sequeira, S., Evtuguin, D. V., Portugal, I. & Esculcas, A. P. Synthesis and characterisation of cellulose/silica hybrids obtained by heteropoly acid catalysed sol–gel process. *Mater. Sci. Eng. C* **27,** 172–179 (2007).

127. Guilherme, M. R. *et al.* Superabsorbent hydrogels based on polysaccharides for application in agriculture as soil conditioner and nutrient carrier: A review. *Eur. Polym. J.* **72,** 365–385 (2015).

128. Crescenzi, V. *et al.* New hydrogels based on carbohydrate and on carbohydrate-synthetic polymer networks. *Polym. Gels Networks* **5,** 225–239 (1997).

129. Guo, M., Jiang, M., Pispas, S., Yu, W. & Zhou, C. Supramolecular Hydrogels Made of End-Functionalized Low-Molecular-Weight PEG and α-Cyclodextrin and Their Hybridization with SiO_2 Nanoparticles through Host–Guest Interaction. *Macromolecules* **41,** 9744–9749 (2008).

130. Shelke, N. B., James, R., Laurencin, C. T. & Kumbar, S. G. Polysaccharide biomaterials for drug delivery and regenerative engineering. *Polym. Adv. Technol.* **25,** 448–460 (2014).

131. Novotna, K. *et al.* Cellulose-based materials as scaffolds for tissue engineering. *Cellulose* **20,** 2263–2278 (2013).

132. Weiss, P. *et al.* Self-Hardening Hydrogel for Bone Tissue Engineering. *Macromol. Symp.* **266,** 30–35 (2008).

133. Lide, D. R., Eleanor Lide David Alston Lide, M. & Grace Eileen Lide David Austell Whitcomb Kate Elizabeth Whitcomb, J. *CRC Handbook of Chemistry and Physics, 84th Edition, 2003-2004*. (2003).

134. Bell, R. P. *The Proton in Chemistry*. (Springer US, 1973). doi:10.1007/978-1-4757-1592-7

135. Atkins, P. W. (Peter W. *Shriver & Atkins' inorganic chemistry*. (Oxford University Press, 2010).

136. Immergut, E. H., Schurz, J. & Mark, H. Viskositätszahl-Molekulargewichts-Beziehung für Cellulose und Untersuchungen von Nitrocellulose in verschiedenen Lösungsmitteln. *Monatshefte für Chemie* **84,** 219–249 (1953).

137. Fardim, P., Holmbom, B. Fast determination of anionic groups in different pulp fiber by methylene blue sorption, Solutions! *TAPPI J.* **2,** (2003).

138. Harned, H. S. & Fleysher, M. H. THE ACTIVITY COEFFICIENTS OF HYDROCHLORIC ACID IN SOLUTIONS OF ETHYL ALCOHOL. *J. Am. Chem. Soc.* **47,** 82–92 (1925).

139. Håkansson, H. & Ahlgren, P. Acid hydrolysis of some industrial pulps: Effect of hydrolysis conditions and raw material. *Cellulose* **12,** 177–183 (2005).

140. Grunwald, E. & Berkowitz, B. J. The Measurement and Correlation of Acid Dissociation Constants for Carboxylic Acids in the System Ethanol-Water. Activity Coefficients and Empirical Activity Functions [1a]. *J. Am. Chem. Soc.* **73,** 4939–4944 (1951).

141. Ma, Y., Loyns, C., Price, P. & Chechik, V. Thermal decay of TEMPO in acidic media via an N-oxoammonium salt intermediate. *Org. Biomol. Chem.* **9,** 5573 (2011).

142. Tsuguyuki Saito & Isogai*, A. TEMPO-Mediated Oxidation of Native Cellulose. The Effect of Oxidation Conditions on Chemical and Crystal Structures of the Water-Insoluble Fractions. (2004). doi:10.1021/BM0497769

143. Isogai, T., Saito, T. & Isogai, A. TEMPO Electromediated Oxidation of Some Polysaccharides Including Regenerated Cellulose Fiber. *Biomacromolecules* **11,** 1593–1599 (2010).

144. Hirota, M., Tamura, N., Saito, T. & Isogai, A. Oxidation of regenerated cellulose with NaClO2 catalyzed by TEMPO and NaClO under acid-neutral conditions. *Carbohydr. Polym.* **78,** 330–335 (2009).

145. Hahne, H. *et al.* Carbonyl-Reactive Tandem Mass Tags for the Proteome-Wide Quantification of N-Linked Glycans. *Anal. Chem.* **84,** 3716–3724 (2012).

146. O'Donovan, L. & De Bank, P. A. A hydrazide-anchored dendron scaffold for chemoselective ligation strategies. *Org. Biomol. Chem.* **12,** 7290–7296 (2014).

147. Jia, Y. & Jarrett, H. W. Method for trapping affinity chromatography of transcription factors using aldehyde–hydrazide coupling to agarose. *Anal. Biochem.* **482,** 1–6 (2015).

148. Zhang, H., Li, X., Martin, D. B. & Aebersold, R. Identification and quantification of N-linked glycoproteins using hydrazide chemistry, stable isotope labeling and mass spectrometry. *Nat. Biotechnol.* **21,** 660–666 (2003).

149. Raddatz, S. *et al.* Hydrazide oligonucleotides: new chemical modification for chip array attachment and conjugation. *Nucleic Acids Res.* **30,** 4793–802 (2002).

150. Liimatainen, H., Suopajärvi, T., Sirviö, J., Hormi, O. & Niinimäki, J. Fabrication of cationic cellulosic nanofibrils through aqueous quaternization pretreatment and their use in colloid aggregation. *Carbohydr. Polym.* **103,** 187–192 (2014).

151. Spoljaric, S., Salminen, A., Luong, N. D. & Seppälä, J. Ductile nanocellulose-based films with high stretchability and tear resistance. *Eur. Polym. J.* **69,** 328–340 (2015).

152. Sunthar, P. Polymer Rheology. in *Rheology of Complex Fluids* 171–191 (Springer New York, 2010).

153. Li, Q., Gong, J. & Zhang, J. Rheological Properties and Microstructures of Hydroxyethyl Cellulose/Poly(Acrylic Acid) Blend Hydrogels. *J. Macromol. Sci. Part B* **54,** 1132–1143 (2015).

154. Katona, J. M. *et al.* Rheological properties of hydroxypropylmethyl cellulose/sodium dodecylsulfate mixtures. *J. Serb. Chem. Soc***,** (2013).

155. Zhang, S., Li, F., Yu, J. & Gu, L. Novel fibers prepared from cellulose in NaOH/thiourea/urea aqueous solution. *Fibers Polym.* **10,** 34–39 (2009).

156. Zhang, S. *et al.* Organic/Inorganic Superabsorbent Hydrogels Based on Xylan and Montmorillonite. *J. Nanomater.* **2014,** 1–11 (2014).

157. Larkin, P. (Peter J. . *Infrared and raman spectroscopy : principles and spectral interpretation*. (Elsevier, 2011).

158. Mao, Y., Zhang, L., Cai, J., Zhou, J. & Kondo, T. Effects of Coagulation Conditions on Properties of Multifilament Fibers Based on Dissolution of Cellulose in NaOH/Urea Aqueous Solution. *Ind. Eng. Chem. Res.* **47,** 8676–8683 (2008).

159. Myllytie, P., Salmi, J. & Laine, J. Chitosan, cellulose, and pH. *BioResources* **4,** 1647–1662 (2009).

160. Cui, Z. *et al.* Ionic interactions between sulfuric acid and chitosan membranes. *Carbohydr. Polym.* **73,** 111–116 (2008).

161. L. Heux, *,†, J. Brugnerotto, †, J. Desbrières, †, M.-F. Versali, ‡ and & Rinaudo†, M. Solid State NMR for Determination of Degree of Acetylation of Chitin and Chitosan. (2000).

162. Hiroyuki Kono, † *et al.* CP/MAS 13C NMR Study of Cellulose and Cellulose Derivatives. 1. Complete Assignment of the CP/MAS 13C NMR Spectrum of the Native Cellulose. (2002).

163. Cheung, R., Ng, T., Wong, J. & Chan, W. Chitosan: An Update on Potential Biomedical and Pharmaceutical Applications. *Mar. Drugs* **13,** 5156–5186 (2015).

ISBN 978-952-12-3790-4